0013-7227/04/$15.00/0
Printed in U.S.A.

Endocrinology 145(1):367–383

doi: 10.1210/en.2003-1068

A Transgenic Mouse with a Deletion in the Collagenous Domain of Adiponectin Displays Elevated Circulating Adiponectin and Improved Insulin Sensitivity

TERRY P. COMBS, UTPAL B. PAJVANI, ANDERS H. BERG, YING LIN, LINDA A. JELICKS, MATHIEU LAPLANTE, ANDREA R. NAWROCKI, MICHAEL W. RAJALA, ALBERT. F. PARLOW, LAURELLE CHEESEBORO, YANG-YANG DING, ROBERT G. RUSSELL, DIRK LINDEMANN, ADAM HARTLEY, GLYNN R. C. BAKER, SILVANA OBICI, YVES DESHAIES, MARIAN LUDGATE, LUCIANO ROSSETTI, AND PHILIPP E. SCHERER

Departments of Cell Biology (T.P.C., U.B.P., A.H.B., Y.L., A.R.N., M.W.R., L.C., Y.Y.D., P.E.S.), Physiology and Biophysics (L.A.J.), Pathology (R.G.R.), Neuroscience (A.H.), Medicine (S.O., L.R.), and Molecular Pharmacology (S.O., L.R.); Institute for Animal Studies (R.G.R.); Department of Medicine, Division of Endocrinology, Diabetes Research and Training Center (S.O., L.R., P.E.S.), Albert Einstein College of Medicine, Bronx, New York 10461; Department of Anatomy and Physiology, Laval Hospital Research Center, School of Medicine, Laval University (M.La., Y.-Y.D.), Québec, Canada; National Hormone and Peptide Program, Harbor-University of California-Los Angeles Medical Center (A.F.P.), Torrance, California 90509; Institute for Virology, Technical University Dresden (D.L.), 01307 Dresden, Germany; and Department of Medicine, University of Wales College of Medicine (G.R.C.B., M.Lu.), Heath Park, Cardiff, United Kingdom CF14 4XN

Adiponectin is a plasma protein expressed exclusively in adipose tissue. Adiponectin levels are linked to insulin sensitivity, but a direct effect of chronically elevated adiponectin on improved insulin sensitivity has not yet been demonstrated. We identified a dominant mutation in the collagenous domain of adiponectin that elevated circulating adiponectin values in mice by 3-fold. Adiponectinemia raised lipid clearance and lipoprotein lipase activity, and suppressed insulin-mediated endogenous glucose production. The induction of adiponectin during puberty and the sexual dimorphism in adult adiponectin values were preserved in these transgenic animals. As a result of elevated adiponectin, serum PRL values and brown adipose mass both increased. The effects on carbohydrate and lipid metabolism were associated with elevated phosphorylation of 5′-AMP-activated protein kinase in liver and elevated expression of peroxisomal proliferator-activated receptor γ2, caveolin-1, and mitochondrial markers in white adipose tissue. These studies strongly suggest that increasing endogenous adiponectin levels has direct effects on insulin sensitivity and may induce similar physiological responses as prolonged treatment with peroxisomal proliferator-activated receptor γ agonists. (*Endocrinology* 145: 367–383, 2004)

ADIPOSE TISSUE SECRETES several circulating proteins that have dramatic effects on carbohydrate and lipid metabolism (1, 2). Two of these peptides, adiponectin and resistin, have recently received considerable attention. Resistin has been implicated as a negative regulator of insulin signaling, whereas the adipocyte-specific protein adiponectin has been implicated as a potent insulin sensitizer (3, 4).

Many studies have found a correlation between insulin sensitivity and elevated adiponectin levels in both humans and experimental animals. For example, type II diabetic patients have lower adiponectin levels than nondiabetic controls, and chronic calorie restriction regimens lead to elevated adiponectin (5). Furthermore, in rhesus monkeys predisposed to type II diabetes, the levels of circulating adiponectin decrease before the onset of hyperglycemia (6).

Abbreviations: AMPK, 5′-AMP-activated protein kinase; BAT, brown adipose tissue; CMV, cytomegalovirus; GDI, GDP dissociation inhibitor; LPL, lipoprotein lipase; MCS, multiple cloning site; NEFA, nonesterified fatty acids; PPARγ, peroxisomal proliferator-activated receptor γ; Tg, transgenic; TG, triglycerides; UCP1, uncoupling protein-1; WAT, white adipose tissue; Wt, wild type.

***Endocrinology* is published monthly by The Endocrine Society (http://www.endo-society.org), the foremost professional society serving the endocrine community.**

Pharmacological studies have shown that recombinant adiponectin suppresses endogenous glucose production by raising hepatic insulin sensitivity, an effect also seen in primary hepatocyte cultures (4, 7). Glucose-lowering effects *in vivo* have also been seen with the globular domain of adiponectin (8).

Two reports recently described mouse models with a disruption of the adiponectin locus (9, 10). Mice lacking adiponectin exhibit earlier onset of diet-induced insulin resistance. Even on a normal laboratory chow diet, both adiponectin −/− and −/+ mice display moderate insulin resistance and impaired free fatty acid clearance. However, the effects of chronically elevated serum adiponectin have not been explored to date due to the limited supply of recombinant full-length material.

These observations suggest that low plasma adiponectin contributes to the pathogenesis of insulin resistance and type 2 diabetes. Therefore, elevating adiponectin values can be viewed as a potentially therapeutic objective. Furthermore, transgenic (Tg) methods using conventional strategies of overexpression have also failed to yield a Tg mouse with endogenously elevated adiponectin. Yamauchi *et al.* (11) expressed a truncated analog of adiponectin in Tg mice that only contains the globular domain. However, this fragment clearly lacks the structural

integrity of circulating adiponectin, and it is thus unlikely that it shares the same physiological properties as the native full-length oligomeric complex. Chronic exposure to a class of peroxisomal proliferator-activated receptor γ (PPARγ) ligands known as thiazolidinediones can also increase serum adiponectin levels (12), but this class of drugs clearly induces pleiotropic effects in multiple tissues.

We discovered that the expression of adiponectin lacking a portion of the collagenous domain has a dominant and specific effect on the secretion of native adiponectin. This mechanism was studied *in vitro* and was used to generate a Tg mouse that exhibited a chronic 3-fold induction of adiponectin in serum. This mouse model is unique in that it displays elevated levels of the native oligomeric adiponectin complexes and preserves the effects seen with sexual maturation and sexual differentiation. Adiponectin in this model is therefore under the same developmental control as adiponectin in wild-type (Wt) mice, except that the basal set-point is approximately 3 times higher in the former. Not only do these mice provide insight into the biogenesis of this fat-specific secretory protein, but they also demonstrate a significant improvement in insulin sensitivity that can be achieved through a relatively modest elevation of the serum levels of this protein.

Materials and Methods

Inducible expression of the adiponectin deletion construct in 3T3-L1 adipocytes

3T3-L1 fibroblasts were infected with the retroviral construct pcz-TetDL011 (13) (Lindemann, D., unpublished observations) containing the adiponectin deletion construct. This is a regulatable retroviral vector based on the rtTA/Tet system (14) and murine leukemia virus. In this vector, an EGFP-Zeocin fusion protein and the rtTA genes are constitutively expressed from a bicistronic encephalomyocarditis virus internal ribosome entry site (EMCV IRES) element containing mRNA driven by the viral long terminal repeat promoter. Adiponectin cDNA is expressed from a *tet*-regulatable cytomegalovirus (CMV) minimal promoter located in opposite transcriptional orientation upstream of the 3′ long terminal repeat. Cells were infected, selected for Zeo resistance, and then differentiated according to standard protocols (15). Induction of the deletion construct was initiated after d 8 of differentiation with various levels of doxycyclin (0–1 μM).

Generation of adiponectin Tg mice

The open reading frame encoding murine adiponectin was subcloned into the multiple cloning site (MCS) of pBluescript. The region encoding amino acids 57–95, containing 13 collagen repeats, was deleted using site-directed mutagenesis. The 5.4-kb aP2 enhancer/promoter sequence (provided by Bruce M. Spiegelman, Dana-Farber Cancer Institute, Boston, MA) was introduced into the MCS region upstream of the cDNA. In addition, the simian virus 40 splice and polyadenylase sequences were introduced into the MCS region downstream of the cDNA. For expression of the full-length protein, the complete open reading frame was inserted into the MCS of pCB7 (gift from J. Casanova, Massachusetts General Hospital, Boston, MA). This vector provides expression from a CMV promoter and contains a human GH terminator sequence. The entire cassettes were excised from both vectors and purified for pronuclear injection into fertilized one-cell murine zygotes from FVB mice (Taconic Farms, Germantown, NY). The embryos were implanted in CD-1 mice (Charles River Breeding Laboratories, Wilmington, MA) at the Transgenic Mouse Facility of the Albert Einstein College of Medicine. Transgenic mice were identified by slot-blot analysis using genomic DNA isolated from the tip of the tail. A fragment containing the simian virus 40 region was radiolabeled and used for hybridization by slot-blot analysis.

Laboratory animals

Mice were housed in groups of two to five in filter-top cages and were given free access to water and Teklad rodent diet no. 8604 (Harlan Teklad, Indianapolis, IN). The colony was maintained in a pathogen-free Association for the Accreditation of Laboratory Animal Care-accredited facility at the Albert Einstein College of Medicine under controlled environment settings (22–25 C; 40–50% humidity; 12-h light, 12-h dark cycle with lights on from 0600–1800). The transgene was propagated in a pure FVB background by mating Tg males with Wt females.

Total RNA isolation, RT-PCR analysis, and Northern blot analysis

Tissue was dissected immediately after sacrifice, snap-frozen in liquid nitrogen, and stored at −80 C. Total RNA was isolated from frozen tissue (−80 C) with TRIzol (Life Technologies, Gaithersburg, MD) according to the manufacturer's protocol. cDNA was prepared from 4 μg RNA using Superscript II, and random hexamers (Invitrogen, Carlsbad, CA). The PCR products were analyzed by gel electrophoresis on 1% agarose and scanned under UV light. Northern blot analysis was performed as described previously (16).

Pulse-chase analysis of adiponectin and resistin secretion in 3T3-L1 adipocytes

Fully differentiated d 8 3T3-L1 adipocytes were pulse-labeled for 10 min in the presence of [^{35}S]methionine and cysteine (NEN Life Science Products, Boston, MA). The labeling medium was then exchanged and washed four times with medium containing excess unlabeled methionine and cysteine, and the cells were kept in that medium supplemented with 10% fetal calf serum for up to 24 h. Tissue culture supernatants were harvested, and cells were lysed at the indicated time points. Both supernatants and cellular lysates were immunoprecipitated with antiresistin and antiadiponectin antibodies and analyzed by SDS-PAGE.

Measurement of specific protein levels in tissue by Western blot

Protein was extracted by immersing frozen tissue in cold buffer [20 mM Tris-HCl (pH 7.5), 5 mM EDTA, 10 mM KCl, and 1 mM phenylmethylsulfonylfluoride] and sonicating for 20 sec. The homogenate was centrifuged at 4 C to separate lipids, lysate, and insoluble material. Lysate infranatant was removed and mixed with sodium dodecyl sulfate to a final concentration of 2% (w/v) and heated to 95 C. After 5 min, lysates were cooled to room temperature and centrifuged again. The supernatant was assayed for protein concentration by bicinchoninic acid (protein assay kit, Pierce Chemical Co., Rockford, IL), and 50 μg were assayed for adiponectin, caveolin-1, or GDP dissociation inhibitor (GDI) content by Western blot as previously described. For protein extractions from liver, the tissue was homogenized in a buffer containing 1% Triton X-100, 60 mM octyl-glucoside, 150 mM NaCl, 20 mM Tris (pH 8.0), 2 mM EDTA, 50 mM sodium fluoride, 30 mM sodium pyrophosphate, 100 mM sodium orthovanadate, and 1 mM phenylmethylsulfonylfluoride and sonicated for 20 sec. The resulting homogenate was centrifuged at 4 C, and the supernatant was assayed for protein content by bicinchoninic acid and processed for Western blotting as described above. The antibodies against GDI were a gift from Dr. Perry Bickel (Washington University, St. Louis, MO).

Measurement of adiponectin levels in plasma by Western blot analysis

Blood samples were obtained from the tail vain of unrestrained conscious animals using heparinized capillary tubes (Fisher Scientific, Fairlawn, NJ). Plasma was stored at −20 C for future measurement. Adiponectin in plasma (3 μl) was measured by Western blot analysis. After SDS-PAGE (12%), proteins were transferred to BA83 nitrocellulose (Schleicher & Schuell, Inc., Keene, NH). Blots were exposed to ^{125}I-labeled rabbit antibody against murine adiponectin and analyzed with a PhosphorImager (Molecular Dynamics, Sunnyvale, CA) using ImageQuant 1.2 software. Each gel contained four standards of purified mouse adiponectin at four different concentrations to ensure linearity and re-

producibility of the signal. Inter- and intraassay variations for adiponectin were less than 10%, and the limit of detection was approximately 5 ng adiponectin (12).

Velocity sedimentation for size separation of adiponectin complexes

Sucrose gradients [5–20% in 10 mM HEPES (pH 8) and 125 mM NaCl] were poured stepwise (5%, 10%, 15%, and 20%) in 2-ml, thin-walled, ultracentrifuge tubes (BD Biosciences, Mountain View, CA) and allowed to equilibrate overnight at 4 C. After layering of the plasma sample on top [diluted 1:10 with 10 mM HEPES (pH 8) and 125 mM NaCl in the case of serum], the gradients were spun at 55,000 rpm for 4 h at 4 C in a TLS55 rotor in a TL-100 table-top ultracentrifuge (Sorvall, Kendro Laboratory Products, Newton, CT). Gradient fractions (150 μl) were retrieved sequentially from the top of the gradient and analyzed by quantitative Western blot analysis. This protocol was described in more detail previously (17).

Percent fat mass

The percent fat mass was determined on the basis of the low partition coefficient of H_2O. A known amount of ^3H_2O was injected into the ip cavity and allowed to equilibrate over 8 h. The distribution of tracer in the aqueous compartment was used to calculate the contribution of the lipid stores to the total body weight. The calculation was made under the assumption that 7.5% of the aqueous volume is occupied by nonlipids that nevertheless exclude the tracer.

Indirect calorimetry

Animals undergoing indirect calorimetry were acclimated to the respiratory chambers for 1 d before the gas exchange measurements. Mice were individually housed in the calorimeter cages, and data on gas exchanges, activity, and food intake were collected for 2–3 d. Indirect calorimetry was performed with a computer-controlled Oxymax open circuit calorimetry system (Columbus Instruments, Columbus, OH). Our instrument comprises 4 respiratory chambers with a stainless steel, elevated, wire floor. Each chamber is equipped with water bottle, food tray connected to a balance, and activity monitor. Oxygen consumption and carbon dioxide production were measured for each mouse at 6-min intervals. Outdoor air reference values were measured after every 10 measurements. Instrument settings were: gas flow rate, 0.5 liter/min; settle time, 240 sec; and measure time, 60 sec. Gas sensors were calibrated daily with primary gas standards containing known concentrations of O_2, CO_2, N_2 (Tech Air, Danbury, CT). A mass flow meter was used to measure air flow. A limited diffusion metal-air battery was used as an oxygen sensor. CO_2 was measured with a spectrophotometric sensor. The respiratory quotient was calculated as the ratio of CO_2 production over O_2 consumption. The energy expenditure (EE) was calculated as follows: $EE = (3.815 + 1.232 \times VCO_2/VO_2) \times VO_2$, where VCO_2 is the expired CO_2 volume (ml/kg·h), and VO_2 is the expired O_2 volume (ml/kg·h).

Magnetic resonance imaging

All images were obtained using a 9.4-Tesla imaging system. Mice were first anesthetized by ip injection with a ketamine/xylazine mixture (0.1 ml/20 g body weight). To quantitatively assess whole body fat and water, each mouse was subjected to a 16-scan pulse-acquire sequence in a 40-mm 1H coil, and spectra, including the water and fat peaks, were obtained and analyzed. For imaging, several datasets of eight slices of 2-mm thickness spanning the whole body were obtained. Imaging was conducted using a 35-mm 1H coil and a routine spinecho pulse sequence (18-msec echo time, 600-msec repetition time, and four-signal averages per scan).

Light and transmission electron microscopy

Adipose tissue was fixed with 2.5% glutaraldehyde/1.2% acrolein in sym-collidine buffer, postfixed with 1% osmium tetroxide, followed by 1% uranyl acetate, dehydrated through a graded series of ethanol concentrations, and embedded in LX112 resin (LADD Research Industries, Burlington VT). One-micron-thick sections were cut on an Ultracut UCT (Reichert, Analytical Instruments, Buffalo, NY), stained with 1% toluidine blue in 1% sodium borate, and viewed on an Axiophot light microscope (Carl Zeiss, Inc., New York, NY). Ultrathin sections were cut on a Reichert Ultracut UCT, stained with uranyl acetate, followed by lead citrate, and viewed on a 1200EX transmission electron microscope (JEOL, Inc., Peabody, MA) at 80 kV. For light microscopy of the orbital fat, the entire skull was formalin-fixed, paraffin-embedded, sectioned, and stained with hematoxylin and eosin. For electron microscopy, adipose tissue was dissected from the intraconal region of the orbit and frozen under high pressure using an EMpact High Pressure Freezer (Leica Microsystems, Solms, Austria). The frozen samples were transferred to a Leica EM AFS Freeze Substitution Unit, freeze-substituted in 1% osmium tetroxide in acetone, brought from −90 C to room temperature over 2–3 d, rinsed in acetone, and embedded in LX112 epoxy resin (LADD Research Industries). Ultra thin sections of 70–80 nm were cut on a Reichart Ultracut UCT, stained with uranyl acetate, followed by lead citrate, and viewed on a JEOL 1200EX transmission electron microscope at 80 kV. Photographs were taken with a Zeiss digital imaging system.

Triglyceride clearance

Mice were weighed at 1000 h and were given 15 μl olive oil/g body weight by gastric gavage. Approximately 20 μl blood were collected at 0, 2, 4, and 12 h and assayed for triglycerides (TG; Sigma-Aldrich Corp., St. Louis, MO) and nonesterified free fatty acids (WAKO Diagnostic Products, Richmond, VA). The mice were denied access to food during the course of the study.

Measurement of tissue lipoprotein lipase (LPL) activity

Enzyme activity in adipose tissue was performed as previously described (18). Briefly, tissue homogenates were incubated with a substrate mixture containing [carboxyl-^{14}C]triolein, and nonesterified fatty acids (NEFA) released by LPL were separated and counted. LPL activity was expressed as microunits (1 mU = 1 μmol NEFA released/h of incubation at 28 C). Data are expressed as LPL activity per gram of tissue. The interassay coefficient of variation (4.1%) was using bovine skim milk as a standard source of LPL.

Measurement of glucose flux

Adult (7- to 10-month-old) male Tg mice and their Wt littermates (30–35 g) were anesthetized with chloral hydrate (400 mg/kg body weight, ip) and catheterized through the right internal jugular vein. The venous catheter was used for infusion while blood samples were collected from the tail vein. Each animal was monitored for food intake and weight gain for 3–4 d after surgery to ensure complete recovery. Euglycemic insulin (1 or 4 mU/kg·min) clamps were performed in conscious catheterized mice as previously described (7). Food was removed for 5 h before beginning the *in vivo* studies. A solution of glucose (10%) was infused at a variable rate as required to maintain euglycemia (6 mM). Mice received a constant infusion of HPLC-purified [^{3}H]glucose (0.1 mCi/min; NEN Life Science Products, Boston, MA) or insulin (1 or 4 mU/min·kg body weight). Thereafter, plasma samples were collected to determine glucose levels as well as [^{3}H]glucose specific activity (at 40, 50, 60, 70, 80, and 90 min). Consecutive samples were used for assessment of plasma insulin levels. Steady state conditions for both plasma glucose concentration and specific activity were achieved by 40 min in these studies. In the final stage, mice were anesthetized (60 mg pentobarbital/kg body weight, iv), the abdomen was quickly opened, and the liver was freeze-clamped *in situ* with aluminum tongs cooled in liquid nitrogen. The time between the injection of anesthesia and the freeze-clamping of tissue samples never exceeded 60 sec. Tissue samples were stored at −80 C for further analysis. The euglycemic clamp protocol was approved by the institutional animal care and use committee of the Albert Einstein College of Medicine.

High fat feeding and oral glucose tolerance tests

A cohort of mice was maintained on a high fat diet from weaning at 3 wk to 6 months of age (59% of calories derived from fat; D12492

Research Diets, Harlan Teklad, Madison, WI). Fasted mice (5 h) were given an oral glucose load (2.5 mg glucose/g body weight using a solution of 10% glucose in physiological saline). Blood was collected at 0, 30, 60, and 120 min and used for glucose (Sigma-Aldrich Corp.) and insulin (Linco Research, St. Charles, MO) measurements. Access to food was denied during the course of the study.

Statistical analysis

Results are shown as the mean ± SEM. Statistical analysis was performed by unpaired *t* test (nonparametric), assuming unequal variance unless otherwise indicated. Significance was accepted at $P < 0.05$.

Results

Adiponectin overexpression

It has been extremely difficult to elevate adiponectin in serum by simple overexpression. Relatively high serum concentrations, a short half-life, and feedback inhibition on endogenous production/clearance may contribute to the complexity. We developed a novel Tg strategy to elevate adiponectin in the circulation using a deletion mutant of adiponectin under control of the adipose-specific enhancer/promoter of the aP2 gene. This deletion mutant lacks 13 of 22 Gly-X-Y repeats in the collagenous domain (Fig. 1A). The strategy was initially developed in tissue culture to elucidate the biogenesis of the adiponectin complex.

Adiponectin forms homotrimers upon translocation into the lumen of the endoplasmic reticulum. The assembly of circulating isoforms of adiponectin begins with a highly stable interaction between the carboxyl-terminal globular domains of three adiponectin subunits and proceeds to the collagenous domain (19). Subsequently, pairs of trimers are linked through the formation of a disulfide bond at Cys^{39} (17). Pairs of trimers ultimately assemble into higher order structures that contain 12 or 18 adiponectin subunits. A deletion mutant of adiponectin lacking 13 of 22 Gly-X-Y repeats in the collagenous domain (ΔGly-adiponectin) interferes with the folding of individual trimer units.

The effects on adiponectin secretion can be inverted based on the expression of full-length to ΔGly-adiponectin. Low ΔGly-adiponectin expression increases the secretion of full-length adiponectin, whereas high levels lower the secretion of full-

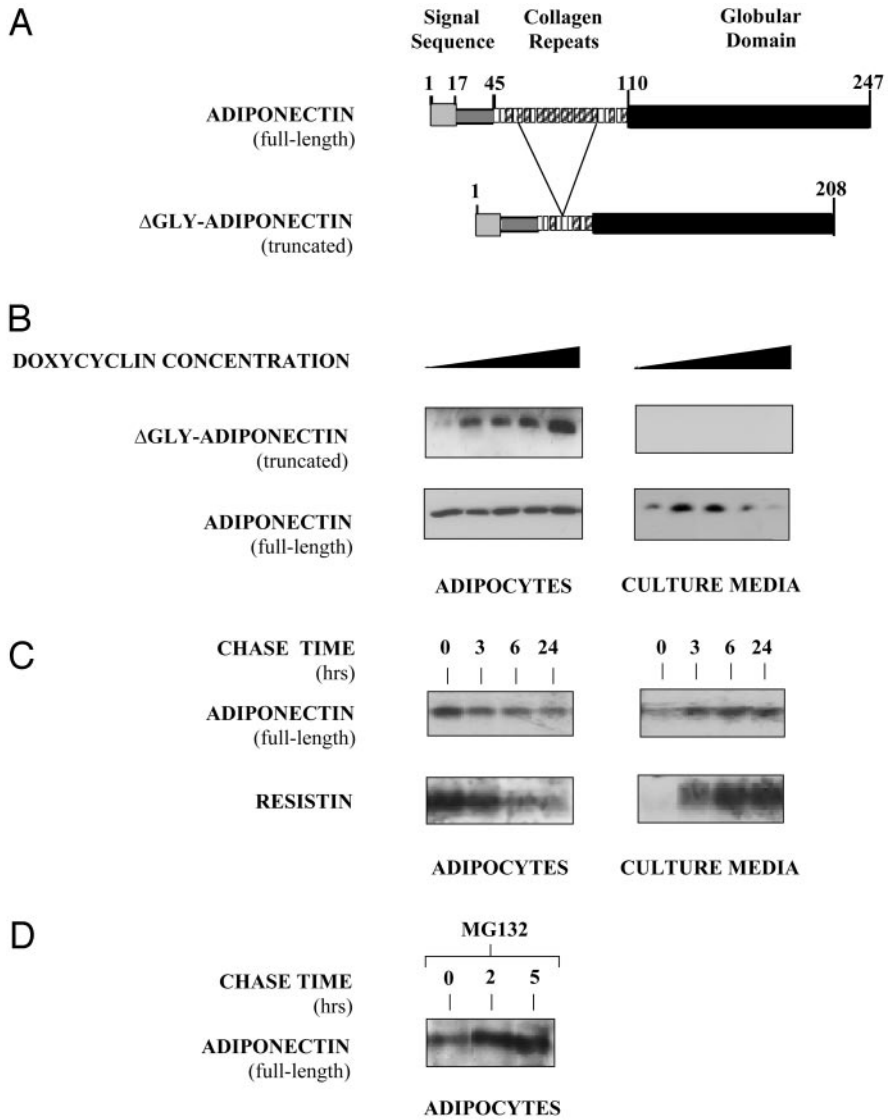

FIG. 1. A, Structural domains of adiponectin and ΔGly-adiponectin; the GlyXY motifs in the collagenous domain are shown in *white* and *hatched bars*. B, Inducible expression of the deletion construct in 3T3-L1 adipocytes. Cells were differentiated according to the standard differentiation protocol. After 8 d, the expression of the deletion construct was induced by the addition of various levels of doxycyclin (0–1 μM). After 72 h, medium was replaced with fresh serum-free medium containing the equivalent amount of doxycyclin. After 18 h, the cell lysates and supernatants were analyzed for adiponectin expression by Western blot analysis under reducing conditions. Note that a longer exposure was required to detect the expression of the intracellular deletion construct. C, Pulse-chase study in 3T3-L1 adipocytes. Cells were pulsed with [^{35}S]Cys/Met as described in *Materials and Methods*. Intracellular and extracellular materials were assayed for the presence of adiponectin and resistin by immunoprecipitation. D, Treatment of 3T3-L1 adipocytes with the proteasomal inhibitor MG132. At the indicated times after initiation of the treatment with 10 μM MG132, cells were lysed and analyzed for intracellular levels of adiponectin by Western blot analysis.

length adiponectin. This was shown in a dose-dependent induction of the mutant protein in 3T3-L1 adipocytes by Western blot analysis under reducing conditions (Fig. 1B). Note that a greater exposure period was needed to detect the intracellular expression of ΔGly-adiponectin compared with full-length adiponectin, and that ΔGly-adiponectin is not secreted under any circumstances. This effect can be exclusively achieved at the level of secretion, as endogenous adiponectin mRNA levels are not altered by ΔGly-adiponectin (data not shown). This is consistent with our previous observations that point to a critical posttranscriptional component in the relationship of sexual dimorphism to adiponectin levels (20). This suggested that a pool of endogenous adiponectin within the secretory pathway of adipocytes could be effectively released through low expression of ΔGly-adiponectin.

More detailed analysis of the secretion kinetics for adiponectin using a pulse-chase study revealed that near-maximal levels of secretion could be achieved within 3 h after initiation of the chase. The remaining material was retained intracellularly and slowly degraded (Fig. 1C). This is in stark contrast to the secretion kinetics of resistin, another adipocyte-specific secretory protein that could be almost quantitatively secreted under the same conditions. The inability of the remaining intracellular adiponectin pool to be released is not a reflection of a high level of misfolding, as a number of treatments (*e.g.* treatment with β_3 agonists or reducing agents) can effectively tap into this intracellular pool and release it (Berg, A., and U. Pajvani, unpublished observations). This suggests that under normal conditions, a futile cycle is in place that is characterized by high level production of adiponectin, followed by degradation of nearly 50% of the newly synthesized material. Degradation most likely involves the cytosolic proteasomal complex, because treatment of cells with MG132, a proteasomal inhibitor, leads to a significant accumulation of intracellular adiponectin, as shown by Western blot analysis in 3T3-L1 cells (Fig. 1D). In the absence of ΔGly-adiponectin, normal basal levels of full-length adiponectin are secreted. Upon low level induction of ΔGly-adiponectin, a small amount of mixed trimers is formed, blocking the futile degradation cycle of the Wt protein. This significantly increases the secretion of full-length adiponectin. At higher levels of the mutant protein, the deletion construct effectively integrates into all trimers formed, thereby quantitatively blocking the secretion of almost all of the full-length adiponectin. The net result of transgene expression is therefore a more efficient secretion of endogenous Wt adiponectin complexes.

Based on our observations in tissue culture, we expressed ΔGly-adiponectin under the control of a fat cell-specific aP2 promoter in mice. Tg mice with Wt adiponectin under control of the more ubiquitously expressed CMV promoter were also generated in parallel. The results from three and four founder lines are shown for both constructs (Fig. 2B). In the case of CMV-adiponectin, a much larger number of founders was analyzed (>30), but they are not shown. RT-PCR analysis of gonadal fat with transgene-specific primers showed three lines expressed ΔGly-adiponectin, but only line 2 had increased circulating levels in serum (Fig. 2C). Because ΔGly-adiponectin females are infertile, the line was propagated through Tg males and Wt females that yielded a Tg birth rate of 50%.

Although several founders expressed the CMV-adiponectin transgene, line 3 had increased serum concentrations of adiponectin. Interestingly, both line 2 of aP2-ΔGly-adiponectin and line 3 of CMV-adiponectin mice developed an unusual phenotype at midlife that included expansion of the interscapular region and bilateral exophthalmia (Fig. 2D). An increase in serum adiponectin correlated with the appearance of this phenotype. The expression of either aP2-ΔGly-adiponectin or CMV-adiponectin without an increase in serum adiponectin did not produce expansion of the interscapular region and exophthalmia in old age (24–30 months).

Line 2 from aP2-ΔGly-adiponectin was chosen for further analysis because it showed the greatest elevation of serum adiponectin. A survey of transgene expression by RT-PCR in various fat pads and other tissues (Fig. 3A) revealed that ΔGly-adiponectin expression under the aP2 promoter overlapped endogenous adiponectin expression and is thus limited to adipose tissue. Adiponectin levels in various fat pads (interscapular, inguinal, mammary, and epididymal) were elevated in both male and female Tg mice. Interestingly, perimetrial (uterine) fat differed from all other fat pads examined in that a reduction of adiponectin was observed in the Tg animals (Fig. 3B). As the clearance of adiponectin was not markedly different in Wt and mutant mice (data not shown), the net increase in serum in Tg mice was primarily due to increased secretion of the protein from a range of adipose pads.

Mice exhibit a marked sexual dimorphism with respect to serum adiponectin levels (20). Males and females displayed a dramatic increase in adiponectin at puberty, and subsequently, adult females exhibited 2- to 3-fold higher levels than adult males. As the expression of ΔGly-adiponectin allowed endogenous adiponectin to escape degradation, the early rise in serum levels and the sexual dimorphism were both preserved in ΔGly-adiponectin mice at an overall higher level. Both male and female ΔGly-adiponectin mice exhibited serum adiponectin levels 3-fold above those in their age- and sex-matched Wt littermates (Fig. 4A).

Adiponectin circulates mainly in two high order forms (17). The relative distribution of these forms may have functional implications. Tg mice displayed a similar distribution of these high order forms as their Wt littermates. Although the levels of adiponectin were increased in Tg mice, the size profile of high order complexes was similar to that of Wt mice (Fig. 4B). This strongly suggests that the complexes generated in Tg mice fold properly and resemble Wt protein in their oligomeric make-up.

Male Tg mice displayed similar body weights as their Wt littermates up to 1 yr (Fig. 4C). Tg females, however, started to weigh significantly more than their Wt littermates around 16 wk of age and continued to be heavier until 1 yr of age when they displayed a small, but significant, 15% increase in overall body mass (Fig. 4C).

Chronic elevation of adiponectin does not affect food intake, but leads to an increase in adiposity in females

At 6–8 months of age, we determined the percent body fat content in males and females. There was a significant in-

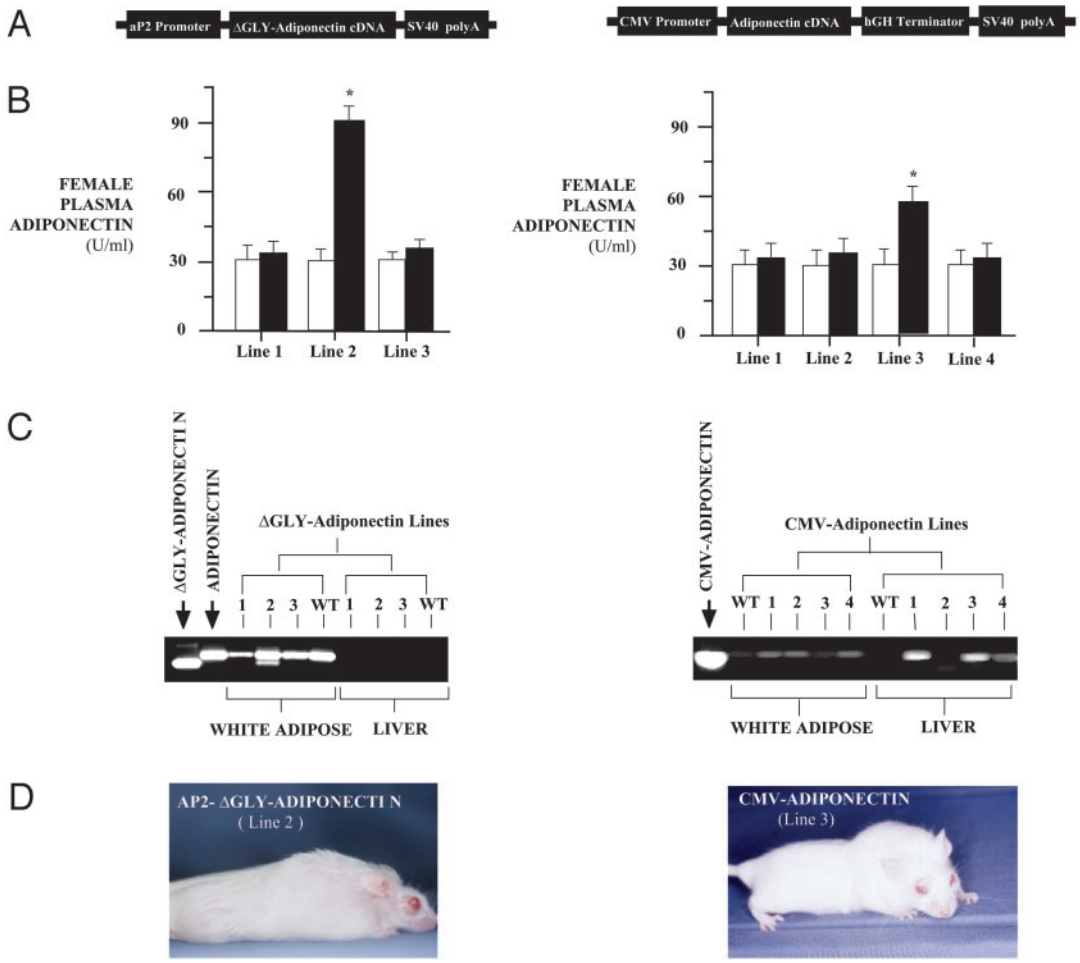

FIG. 2. A, Tg expression constructs for 1) truncated adiponectin lacking seven GlyXY repeats (ΔGly-adiponectin) under the adipocyte-specific aP2 promoter (*left*), or 2) full-length adiponectin under the ubiquitous active CMV promoter (*right*). B, Plasma adiponectin levels of Wt adiponectin resulting from Tg expression of aP2-ΔGly (*left*) or CMV-adiponectin (*right*). □, Female Wt mice; ■, female Tg littermates. The levels are indicated as arbitrary densitometric units. C, Transgene expression assessed by nonquantitative RT-PCR using primers that recognize the endogenous Wt adiponectin and the ΔGly construct (*left*) or primers specific for the CMV-adiponectin transgene (*right*). D, Phenotypic appearance of Tg mice: expansion of interscapular tissue in 12-month-old mice carrying the aP2-ΔGly transgene (*left*) or the CMV-adiponectin transgene (*right*).

crease in percent total body fat by that age in the females, which reached approximately 30% of their total body weight, in contrast to 18% in their Wt siblings (Fig. 5A). The males did not display any significant differences at that age (data not shown). These differences in the females could not be explained by a difference in food intake within the accuracy with which these experiments can be performed (Fig. 5B). We were also unable to observe any changes with respect to the average 24-h energy expenditure (Fig. 5C), nor were there differences with respect to the respiratory quotient in either the resting or the active state (Fig. 5D).

Chronic elevation of adiponectin leads to remodeling of select fat depots

Even though a detailed pathological examination of the mice did not reveal any gross morphological changes, it became apparent that Tg female mice developed a large tissue mass in the interscapular region by 12 months (Fig. 6A) that was particularly striking in a cross-sectional view (Fig. 6B). Magnetic resonance imaging strongly suggested that the expansion consists primarily of lipid mass (Fig. 6B). A histological analysis at the light microscopic (Fig. 6C) and electron microscopic (Fig. 6D) levels clearly identified the expanding tissue mass as adipose tissue. Interscapular brown adipose tissue (BAT) could be identified in both Wt and Tg mice on the basis of its darker brown appearance. Rather than the classical multilobular appearance of the lipid droplets as they appeared in Wt mice, the Tg BAT had a more unilocular appearance.

Another fat pad that selectively hyperproliferates is the orbital (intraconal) fat pad. This was evident in 100% of 12-month-old females. Orbital fat proliferation pushed the orbit away from the shallow bony orbit, producing axial proptosis. The proptosis progressed asymmetrically, but eventually affected both eyes (Fig. 7A). High resolution magnetic resonance imaging (Fig. 7B) and histological analysis (Fig. 7C) clearly indicated the intraconal fat pad as the primary cause of the proptosis. There was no indication of

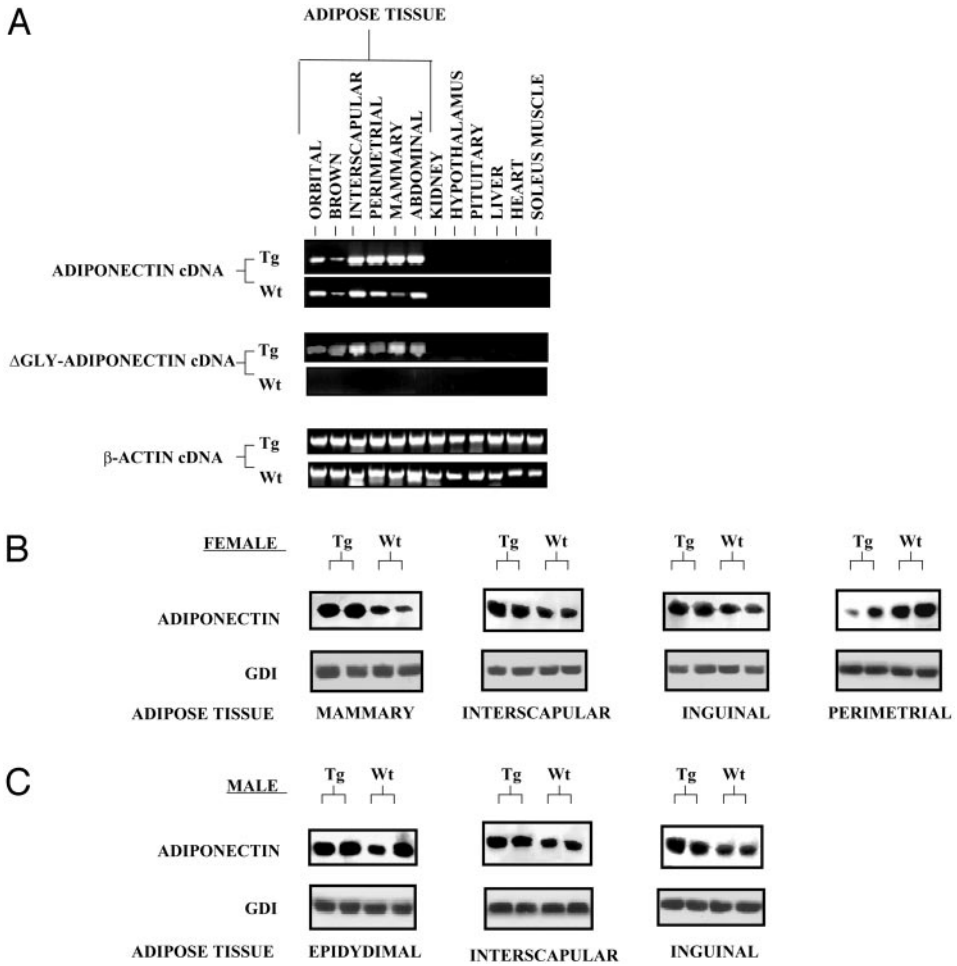

FIG. 3. A, Tissue profile for mRNA expression of adiponectin, the adiponectin transgene (ΔGly-adiponectin), and β-actin expression in female ΔGly-adiponectin mice (Tg) and their Wt littermates (Wt) by RT-PCR analysis. B, Western blot analysis for adiponectin levels in adipose tissue from 4-month-old female (*left*) and male (*right*) Tg mice and their Wt littermates. BAT and inguinal and mammary/epididymal WAT were used; representative extracts from two mice per group are shown. Equal protein loading was confirmed by blotting for the internal standard GDI.

immune infiltration or inflammatory activity within the muscle fibers, but individual orbital muscles separated into multiple fibers by the expansion of adipose tissue. At the orbital apex, the tendinous ring insertion of the ocular muscles dilated as fat prolapsed. Chronic exposure keratopathy due to proptosis ultimately ulcerated the entire cornea and resulted in globe perforation with hemorrhagic ulcerated plaque clinging to the sclera beneath, followed by complete globe shrinkage and fibrosis (phthisis). The intraconal fat further expanded between the straps of ocular muscles. The proptosis worsened progressively and mice were usually euthanized by 15 months of age.

This selective expansion of the orbital adipose tissue is reminiscent of pathological changes associated with some cases of Graves' disease (21). However, our results suggest that it is unlikely that overexpression of adiponectin triggers an autoimmune reaction toward the TSH receptor as observed in Graves' patients, because TSH receptor antibodies were assayed using three different methods that measure 1) simple binding to the TSH receptor; 2) TSH receptor agonist activity, resulting in elevated intracellular cAMP; and 3) inhibition of binding of the endogenous TSH receptor ligand, TSH. No evidence for a humoral autoimmune reaction to the TSH receptor was observed (Table 1).

Both Wt and Tg orbital adipocytes have multiple mitochondria and express the BAT-specific marker protein uncoupling protein-1 (UCP1; Fig. 7D). The primary source of expanding fat in Tg mice therefore appears to originate from BAT-like tissue, as judged by low level UCP1 expression even in Wt fat (Fig. 7E). This adipose mass expanded laterally, eventually wrapping around the entire neck. With age, the adipose tissue stretched even further and included regions of the head, including the submandibular fat pad (see three-dimensional nuclear magnetic resonance movie of Wt and Tg published as supplemental data on The Endocrine Society's Journals Online web site, http://endo.endojournals.org).

Macroscopic appearance and weight were comparable between Wt and Tg in all other adipose pads examined. The expansion of the interscapular and orbital adipose tissues was significantly delayed in males.

Chronic elevation of adiponectin affects PRL levels

Serum levels of adiponectin are under complex hormonal control (20). To test whether chronic adiponectin overexpression feeds back on any factors known to affect adiponectin levels under normal conditions, we determined serum levels of a number of hormones and metabolites. Table 2 shows that levels of TNFα and glucocorticoids were normal; the pituitary hormones GH and TSH were also comparable in Wt and Tg. Surprisingly, despite overall increased fat mass in Tg females, leptin levels were comparable as well. In

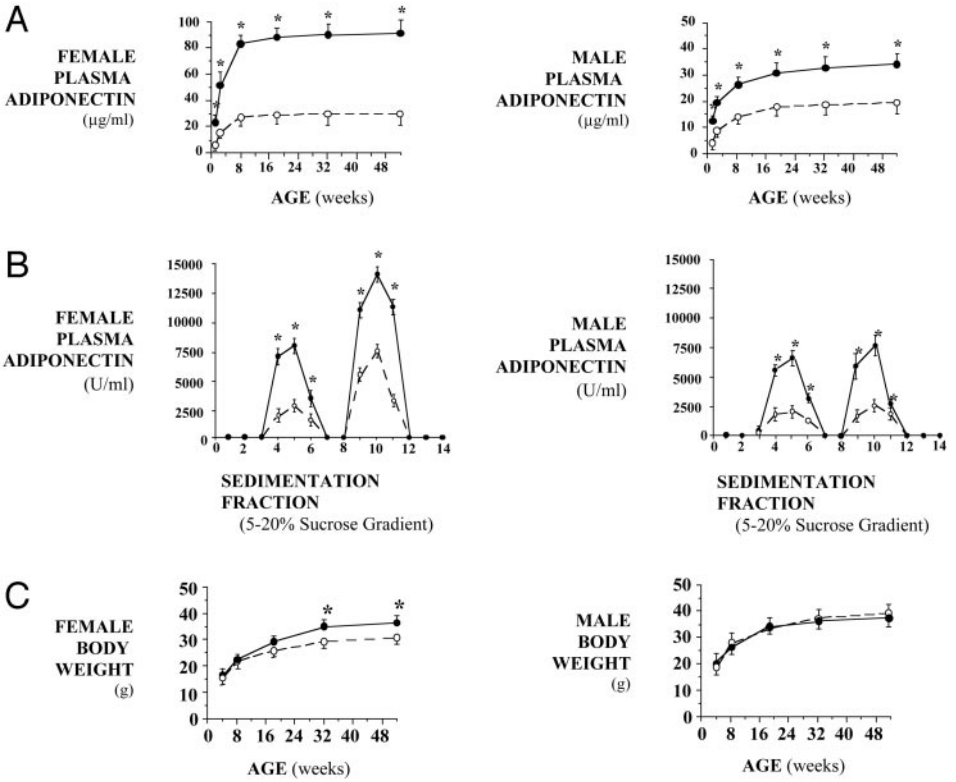

FIG. 4. A, Circulating adiponectin levels in female (*left*) and male (*right*) ΔGly-adiponectin (Tg) mice (●) and their Wt littermates (○) measured in a longitudinal 1-yr study by Western blot analysis. B, Size distribution of circulating adiponectin in 4- to 6-month-old female (*left*) and male (*right*) Tg mice (●) and their Wt littermates (○) using velocity sedimentation in 5–20% sucrose gradients. The numbers reflect arbitrary densitometric units per milliliter of plasma. C, Change in body weight of female (*left*) and male (*right*) Tg mice (●) and their Wt littermates (○) during a longitudinal 1-yr study. Each group represents 8–10 mice. *, $P < 0.05$, Wt *vs.* Tg mice.

contrast, Tg males and females displayed a 2-fold increase in PRL levels. PRL exerts a strong negative influence on serum adiponectin levels in Wt mice (20). The chronic elevation of PRL levels in Tg animals may therefore reflect a compensatory mechanism to lower the elevated concentration of adiponectin in serum.

Improved clearance of TG in female Tg adiponectin mice

Several groups have proposed an involvement of adiponectin in TG and free fatty acid metabolism (8). To test whether there is an effect on TG clearance, we gavaged a group of Wt and Tg mice with olive oil and monitored TG and free fatty acid levels in plasma during the subsequent 12 h. Tg females displayed dramatically different clearance rates than Wt mice. Plasma TG and free fatty acid (NEFA; Fig. 8, A and B) levels before the gavage were vastly overlapping. However, subsequent to the gavage, plasma levels of TG and NEFAs were consistently lower in the Tg animals, never approaching the peak levels found in Wt females. These observations suggest that chronically increased levels of adiponectin in females have a positive impact on TG clearance and are consistent with acute pharmacological effects that lead to a decrease in plasma TG upon injection of recombinant adiponectin. The more modest increases in serum adiponectin levels in males are not sufficient to cause any changes in lipid clearance, because the kinetics of TG and NEFA disposal are vastly overlapping between Wt and Tg males. A partial explanation for this effect is revealed upon analysis of adipose tissue lipoprotein lipase activity (Fig. 8C). The Tg females displayed significantly elevated LPL activity per gram of tissue in the fed state in a number of different fat pads. Similar trends were observed in the fasted state (not shown). Consistent with the improved clearance of TG that could only be observed in females, the increased lipoprotein lipase activity was observed in females only. Additional metabolic parameters were analyzed in these mice, but did not reveal any significant differences (Table 3).

Chronic increase in serum adiponectin triggers transcriptional changes in adipose tissue

To describe the changes in the signaling modules involved in insulin signal transduction more fully we analyzed adipose tissue extracts by Western blot analysis. We previously reported that mice with a genetic deletion of the caveolin-1 locus display a reduction of serum adiponectin by almost 90% (22). Caveolin-1 is a critical regulator of signal transduction and has also been implicated as a modulator of insulin receptor signaling. The association between adiponectin and caveolin-1 levels is preserved in this Tg model as well. Adipose pads with increased production of adiponectin [BAT and mammary white adipose tissue (WAT) are shown as representative examples] showed increased caveolin-1 levels, whereas metrial fat that showed reduced levels of adiponectin in the Tg mice also had reduced levels of caveolin-1 (Fig. 9A).

Finally, as many of the phenotypes described for the Tg mice are consistent with increased PPARγ activation, we tested whether we would detect increased PPARγ2 levels in Tg mice. At least in a subset of white fat pads (Fig. 9B shows abdominal fat as a representative example), PPARγ2 mRNA levels were markedly increased, particularly in females. Fur-

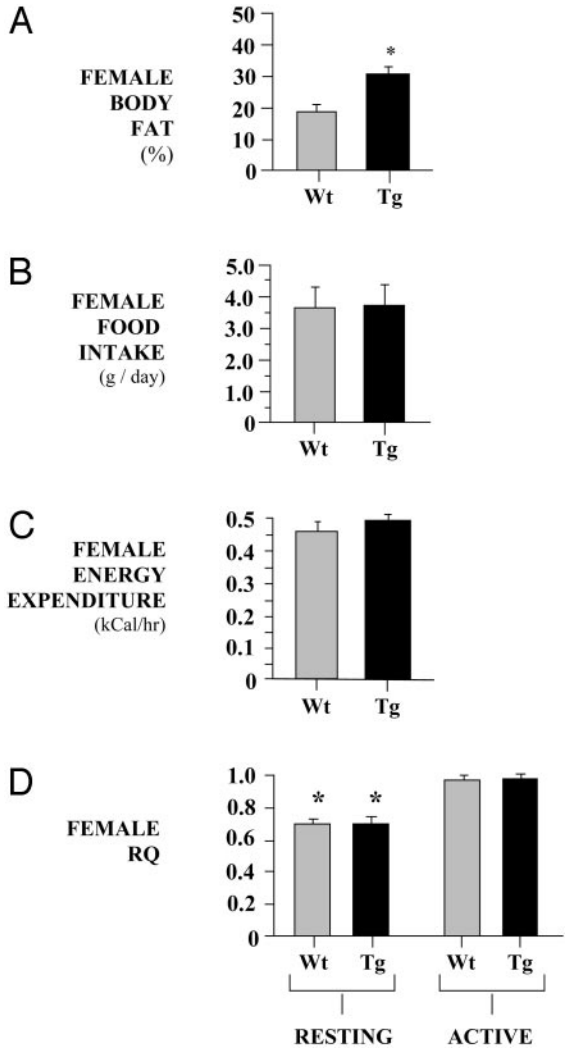

FIG. 5. Comparison of energy homeostasis between female Wt and ΔGly-adiponectin (Tg) mice at 8 months of age. Percent body fat (A) and daily food intake (B) of 8-month-old individually housed Wt and mice and their Tg littermates. The percent body fat was determined by equilibration of ^3H_2O. Energy expenditure (C) and respiratory quotient (D) in the resting and active states were obtained by indirect calorimetry in 8-month-old female Tg mice (■) and their Wt littermates (▨). Gas exchanges were measured in mice individually housed in metabolic chambers, whereas activity was monitored with an infrared light movement sensor. Resting values for energy expenditure were calculated from measurements obtained during times when activity sensors recorded less than 20 events in a 20-min interval. Gas exchanges values were the mean of measurements made every 20 min for a 24-h period after a 24- to 48-h acclimation period. Each group represents 8–10 mice. *, $P < 0.05$, active is significantly higher than resting.

thermore, resistin mRNA levels were slightly induced compared with control levels, and a very significant induction of mRNA levels of several mitochondrial markers (the ADP/ATP translocator and the dicarboxylate transporter are shown) was detected.

Euglycemic insulin clamps reveal dramatically improved hepatic insulin action in Tg adiponectin mice

To determine whether chronic increases in circulating levels of adiponectin improve glucose tolerance by increasing glucose uptake, decreasing glucose production, or both, we used the insulin clamp technique on a cohort of 7- to 10-month old male and female mice that were fed a standard laboratory chow diet. Insulin infusion rates were selected to raise plasma insulin levels similarly in all groups, and a variable infusion of a 10% glucose solution was started and periodically adjusted to maintain the plasma glucose concentration at approximately 5 mM for the rest of the study. Similar to the acute administration of recombinant adiponectin, the rate of disappearance of glucose was not altered in Tg mice, indicating that whole body glucose uptake was not affected. However, with either low (1 mU/kg·min) or high (4 mU/kg·min) insulin, glucose production in Tg females was lower than that in Wt mice, indicating greater insulin sensitivity in the Tg animals (Fig. 10, A and B). This effect became even more striking with hyperinsulinemia, which demonstrated a marked decrease in the rates of glucose production in Tg animals compared with Wt mice in both females and males (Fig. 10B). Therefore, both male and female Tg mice exhibit increased hepatic insulin sensitivity. The relevant metabolic parameters for these experiments are indicated in Table 4. From that table it is apparent that the Tg mice displayed a marked decrease in postabsorptive plasma insulin concentrations compared with Wt mice. Although female Tg mice do show initial signs of increased interscapular fat mass at this age, it is important to note that the males do not display any detectable differences in fat distribution between Wt and Tg animals, emphasizing that the improvement in hepatic insulin sensitivity is not a consequence of the interscapular fat hyperproliferation.

Kadowaki and colleagues (23) have recently shown that full-length adiponectin activates 5′-AMP-activated protein kinase (AMPK) in liver. We therefore examined the activation state of AMPK in livers isolated from female animals used for the hyperinsulinemic clamp studies. Although absolute AMPK levels were not different, and basal phospho-AMPK levels were very low in Wt and Tg animals, Tg animals displayed a prolonged activation of AMPK that could still be visualized at the end of the clamp studies (Fig. 10C), consistent with our own observations in primary hepatocytes upon treatment with adiponectin (not shown) and *in vivo* results by other groups (23), further corroborating that elevated adiponectin levels will lead to activation of AMPK.

Elevated circulating adiponectin improves oral glucose tolerance

Our previous studies suggested that pharmacological levels of recombinant adiponectin dramatically improve hepatic insulin sensitivity in Wt and type I and type II diabetic mice. To further test whether the constitutively elevated adiponectin levels in our Tg mice have an impact on insulin sensitivity, we subjected a cohort of high fat-fed Wt and Tg males to an oral glucose tolerance test. The presence of the transgene did not prevent weight gain during a high fat diet for 6 months. A modest increase in body weight was observed in female Tg compared with their Wt littermates, similar to chow-fed animals (Fig. 11A). The Tg females responded with a significantly improved glucose excursion during an oral glucose tolerance test, indicating improved insulin sensitivity com-

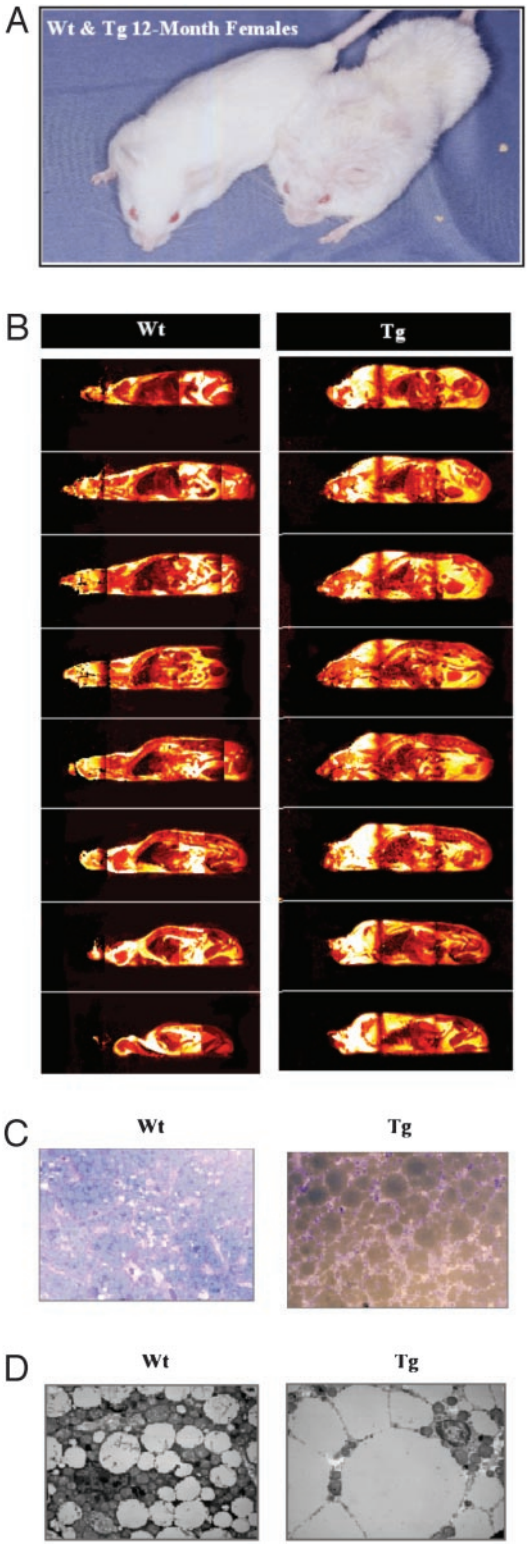

FIG. 6. A, Comparison of a Wt mouse (*left*) and a ΔGly-adiponectin animal (*right*) at 12 months of age. B, Whole body sagittal series of 14-month-old female Wt (*left*) and Tg (*right*) mice obtained by T1 weighted magnetic resonance imaging (MRI). C and D, Light and electron micrographs of interscapular BAT of a 14-month-old female Wt (*left*) and a Tg (*right*) mouse exhibiting hypertrophy of interscapular adipose tissue. Note the increased lipid droplet size in the Tg adipose tissue.

pared with Wt littermates (Fig. 11B). Although glucose disposal was comparable between Wt and Tg, the males not only displayed reduced insulin levels in the basal state, but also achieved normal glucose disposal with significantly lower insulin levels. Female Tg demonstrated improved glucose clearance compared with Wt littermates and required less insulin to achieve these improved clearance kinetics (Fig. 11C). This indicates that the Tg animals are vastly resistant to diet-induced decreases in insulin sensitivity.

Discussion

We have studied the effects of a life-long elevation in circulating adiponectin. To achieve this, we employed a Tg approach that improves the efficiency with which endogenous adiponectin is secreted. In parallel, we have generated a large number (>30) of additional Tg founder lines that express the full-length protein under the control of the ubiquitously expressed CMV promoter. However, only 1 of these lines displayed approximately 3-fold increased serum adiponectin levels, and we were unable to propagate the line due to fertility problems. Interestingly, though, as the first generation of these mice aged, they also displayed hyperproliferation of the interscapular fat pad and the exophthalmos. Again, this phenomenon was not seen in other lines that effectively expressed the CMV-driven transgene, but was strictly dependent on a net increase in serum adiponectin levels.

Epidemiological studies in humans and animal models describe a close association between insulin sensitivity and adiponectin levels within a 2- to 3-fold range from baseline. Consistent with the effects of a pharmacological 2- to 3-fold elevation of adiponectin after the injection or infusion of recombinant adiponectin (4, 7), congenital elevation of adiponectin led to improved hepatic insulin sensitivity. Female Tg mice exhibit a significant increase in the rate of oral lipid clearance, consistent with the phenotype reported for mice carrying a genetic deletion of the adiponectin locus, which display delayed clearance of free fatty acids after injection of a TG emulsion. A recent study by Matsuzawa and colleagues (9) in adiponectin$^{-/-}$ mice focuses on a mechanism involving free fatty acid uptake and oxidation by muscle in line with original suggestions by Lodish and colleagues (8). Although this represents a potential mechanism, we are also intrigued by the effects of adiponectin overexpression on serum TG clearance. It will be interesting to determine whether adiponectin has additional effects on lipolysis or lipoprotein clearance by the liver, perhaps via the same mechanisms as those responsible for the liver glucose effects. Additionally, we reported (22) that mice lacking caveolin-1 display dramatically reduced adiponectin levels coupled with severely elevated TG and free fatty acid levels, especially in the postprandial state. In light of the findings presented here, this suggests that the postprandial hypertriglyceridemia may be functionally related to the reduced adiponectin levels in the caveolin-1$^{-/-}$ mice. It is intriguing that the lack of caveolin-1 triggers reduced adiponectin levels in serum, whereas the Tg up-regulation of adiponectin in Wt mice causes increased adipose caveolin-1 expression. The dramatically increased lipoprotein lipase activity that we

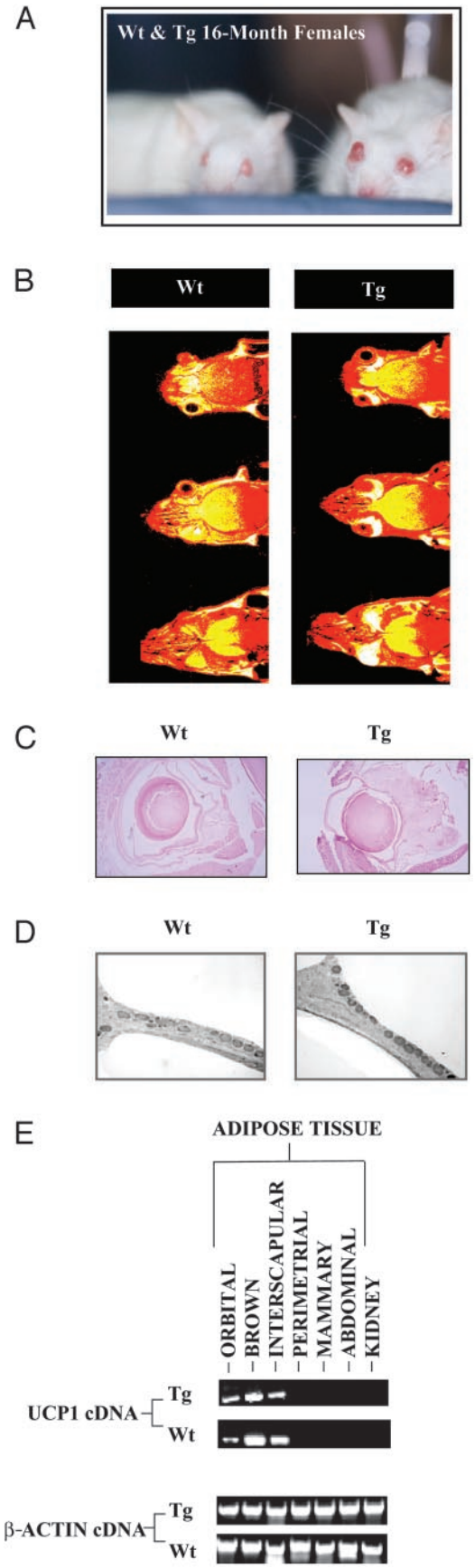

TABLE 1. Antibodies to the thyrotropin receptor (TSHR)

	12- to 16-month-old females	
	Wt	Tg
TSHR IgGs	0.24 ± 0.4	0.22 ± 0.5
TBII	117 ± 3	104 ± 5
TSAB	1.0 ± 0.1	1.2 ± 0.2
TOTAL T_4 (mg/dl)	2.5 ± 0.4	1.8 ± 0.2
TSH (mU/ml)	4.3 ± 0.4	4.5 ± 0.5

CHO cells stably transfected with the human TSHR and flow cytometry were used to measure TSHR IgGs. Mouse serum (diluted 1 in 50) was tested on CHO cells with and without TSHR and the histograms compared using Kolmogorov Smirnof statistics to obtain a "d" value. Two monoclonal antibodies against the TSHR had d values of 0.5 and 0.67, whereas controls with just the second FITC conjugate and no first antibody had a value of 0.24.

Thyrotropin binding inhibiting Igs (TBII) used CHO cells that express TSHR to compare the binding of I-125 TSH in the presence of each individual mouse serum (all in triplicates that agree to within 10%). Results are expressed as a percentage and SE from the average of the counts of the 10 female Wt mice used to define our 100%, *i.e.* no inhibition of I-125 TSH binding. Note that with an excess TSH the binding drops to 25%. Thyroid stimulating antibodies (TSAB) used CHO cells with the TSHR and a cAMP responsive luciferase reporter. Results are expressed as a stimulation index (S.I.) calculated from the ratio of light in the presence of test serum to light in the presence of a euthyroid pool (all tested as duplicates that agree to within 12%). We used the average of the female Wt mice and an S.I. of 1.5 or above is considered positive. Two animals, a transgenic female and male, had weakly positive TSAB. Note that a known human TSAB had S.I. of 3.9, whereas TSH had 20.15.

A total of four to six mice were tested in each case.

observe in female adipose tissues analyzed could contribute to increased clearance of a postprandial TG load. Similar increases in LPL activity have recently been reported in PPARγ agonist-treated rats and linked to improvements in postprandial TG clearance (18).

Humans and mice display a sexual dimorphism for circulating adiponectin values, with female levels increased compared with those in males. This sexual dimorphism is preserved in Tg mice, with the transgene effectively amplifying the host's endogenous levels. Due to overexpression, Tg male mice have levels of adiponectin approximately equal to those in Wt females. The serum concentrations found in Tg males are therefore physiological and readily found in Wt mice, albeit in a different (female) hormonal milieu. Female Tg have levels approximately 3-fold above those in Wt females. Relatively small changes in serum adiponectin concentrations can have a significant effect on insulin sensitivity. An example is seen in heterozygous mice (+/−) with only one functional allele for adiponectin. These mice have approximately 40% of the Wt adiponectin serum levels, but

FIG. 7. A, Frontal view of 11-month-old ΔGly-adiponectin (Tg) and Wt mice with asymmetric exophthalmos. B, MRI series of the head (coronal sections) of a 14-month-old female Wt mouse (*top*) and a Tg mouse (*bottom*). Bright tissue indicates selective hyperplasia of retroorbital adipose tissue in the Tg. C, Light microscopy of the entire orbital cavity after hematoxylin/eosin staining in a 14-month-old female Wt mouse (*left*) and a Tg animal (*right*). D, Intraconal (retroorbital) adipocytes seen by transmission electron microscopy showing a high number of mitochondria in both Wt and Tg. E, UCP1 and β-actin expression in 12-month-old female Tg and Wt mice exhibiting selective hyperplasia of interscapular and intraconal (eye) adipose tissue by nonquantitative RT-PCR analysis. Note the presence of UCP1 in fat pads from Wt mice.

TABLE 2. Serum metabolites in 6- to 8-month-old female and male Wt and ΔGLY-Adiponectin (Tg) mice where n = 5–10 per group in a controlled environment

	6- to 8-month-old females		6- to 8-month-old males	
	Wt	Tg	Wt	Tg
Fed glucagon (mEq/liter)	110 ± 10	105 ± 14	85 ± 13	109 ± 14
Fasted glucagon (mEq/liter)	229 ± 42	289 ± 31	182 ± 34	230 ± 26
Fed corticosterone (mg/dl)	30 ± 4	28 ± 3	18 ± 3	20 ± 2
Fasted corticosterone (mg/dl)	140 ± 15	155 ± 18	118 ± 7	127 ± 12
Prolactin (mEq/liter)	2.4 ± 1.5	*10.9 ± 4.1	7.5 ± 2.2	*11.8 ± 2.0
GH (mEq/liter)	3.7 ± 0.6	5.2 ± 2.2	3.3 ± 0.75	5.5 ± 1.2
Leptin (ng/dl)	4.1 ± 0.4	3.5 ± 0.5	3.3 ± 0.75	3.9 ± 0.5
TNFα (ng/ml)	8.1 ± 1.3	6.7 ± 1.2	3.9 ± 0.6	3.5 ± 0.3

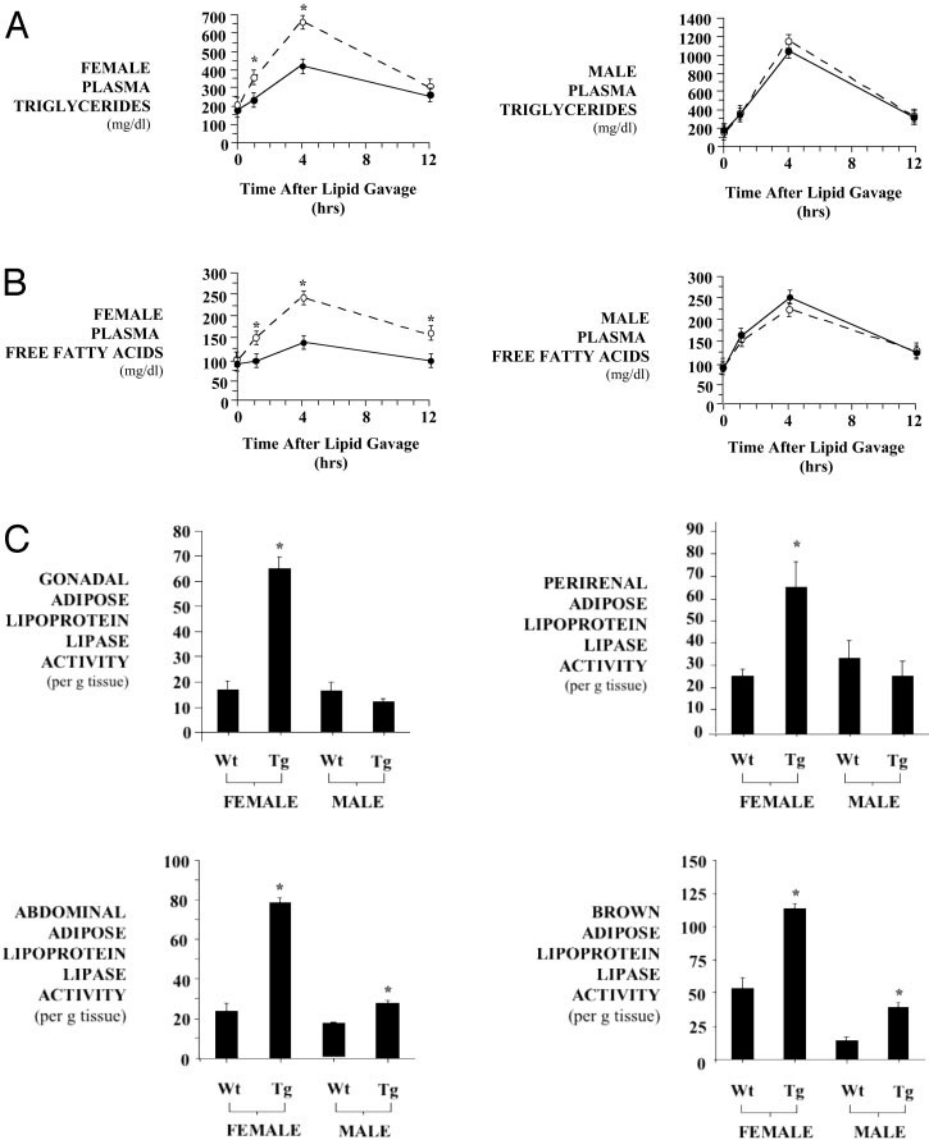

FIG. 8. Circulating TG (A, *top*) and free fatty acids (B, *bottom*) in 6- to 8-month-old female (*left*) and male (*right*) ΔGly-adiponectin mice (●) and their Wt littermates (○) after oral lipid challenge. Mice were kept on a standard chow diet. C, Adipose tissue LPL activity in the fed state in gonadal, perirenal, abdominal, and brown adipose tissue. Note the marked increase in the female Tg animals. Each group represents five animals. *, $P < 0.05$, Wt *vs.* Tg mice.

they have a significantly reduced insulin sensitivity (10). Wt females with higher circulating adiponectin levels are more insulin sensitive than Wt males (20). Acute injections that alter circulating levels by as little as 2-fold have a profound impact on insulin sensitivity (4, 7).

Finally, a number of epidemiological studies in humans that draw strong positive correlations between insulin sensitivity and adiponectin levels focus on values that vary by less than 2- to 3-fold from baseline. Along with the sexually dimorphic expression pattern, we observed various sexually dimorphic phenotypes in a number of different areas. By midlife, the female Tg mouse exhibits a moderate increase in

body weight due to a dramatic increase in interscapular adipose mass. The expansion of interscapular and orbital adipose tissues is also apparent in males older than 20 months. We previously showed that estrogen represses serum adiponectin levels (20) and that ovariectomy results in a significant increase in adiponectin levels in Wt mice. Interestingly, consistent with our hypothesis that the expansion of interscapular and orbital adipose pads is a direct consequence of increased serum adiponectin levels, ovariectomy accelerated the remodeling of fat tissue in the Tg by 3–4 months (data not shown).

Based on the reports by Fruebis *et al.* (8) that increased levels of the globular domain of adiponectin lead to increased β-oxidation in muscle, we suspected that overexpression of adiponectin might lead to a lean phenotype. This is clearly not the case. There is overall an increase in fat mass in females and relatively normal levels in males. Indirect calorimetry confirmed that there is no evidence for an increased metabolic rate in these mice. Importantly, the studies by Fruebis *et al.* (8) focused primarily on the effects of the globular domain, whose pharmacological activities become increasingly more established. However, this globular domain, a putative proteolytic fragment, is difficult to visualize *in vivo*, and it is not clear at this stage whether this fragment is a *bona fide* processing intermediate or represents a pharmacological antagonist only. We have also not been able to detect any specific adiponectin degradation products in the Tg mice with either amino- or with carboxyl-terminal-specific antibodies. We cannot exclude the possibility that there is a rate-limiting step along the activation pathway that we do not overcome by mere overexpression of the full-length product. Nevertheless, the overproduced material in Tg mice is, by all possible criteria established to date, identical to endogenous adiponectin observed under normal conditions. Adiponectin in serum of Tg mice forms complexes of similar molecular weight as adiponectin in Wt mice, with discrete trimer-dimers and a high molecular weight complex. However, based on the data presented, it is clear that overexpression of full-length adiponectin is sufficient to cause marked improvement of insulin sensitivity in liver. Yamauchi *et al.* (11) recently reported overexpression of the globular adiponectin fragment from a liver-specific promoter. When analyzed in a leptin-deficient *ob/ob* background, these mice displayed increased expression of enzymes involved in β oxidation and energy dissipation (such as uncoupling proteins), but did not display decreased adipose mass due to a compensatory increase in food intake. Even though these effects of the globular domain of adiponectin are well established, data from a number of different laboratories indicate the fundamentally different nature of this globular domain compared with the full-length protein found *in vivo*.

Consistent with a recent report by Kadowaki and colleagues (23) demonstrating activation of AMPK by full-length adiponectin in the liver, we observed increased activation of AMPK in our Tg mice at the end of the clamp studies. This further corroborates the functional link between increased adiponectin levels in serum and AMPK activation in the liver.

Yokota *et al.* (24) reported that bacterially produced recombinant adiponectin blocked fat cell formation in long-term bone marrow cultures and inhibited the differentiation

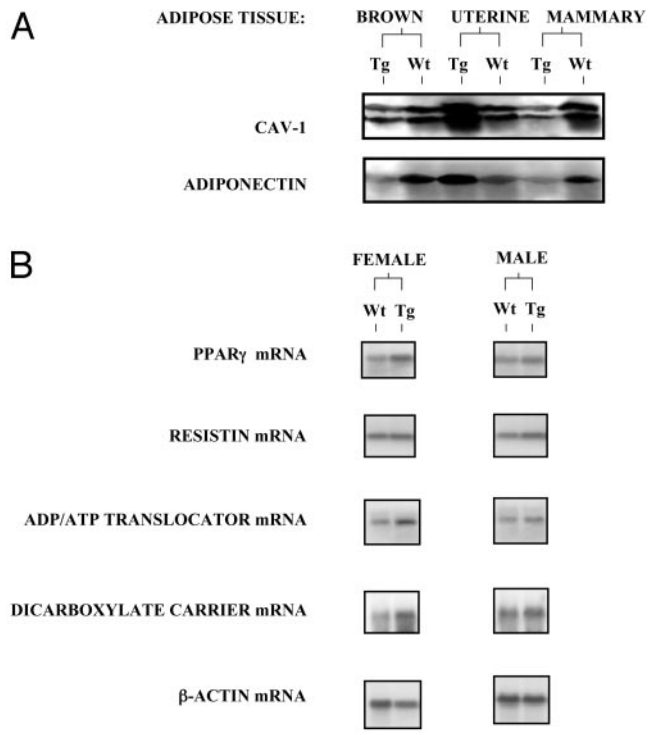

FIG. 9. A, Western blot analysis of caveolin-1 and adiponectin expression in fat pads isolated from Tg and Wt mice. Protein (50 μg) isolated from the respective fat pads was used for analysis. The figure shows a representative Western from three independent experiments. B, Northern blot analysis of female and male abdominal adipose tissues for PPARγ, resistin, the mitochondrial ADP/ATP translocator, and the mitochondrial dicarboxylate carrier mRNA levels. Blots were also probed with β-actin as a loading control. The figure shows a representative Northern blot from three independent experiments.

TABLE 3. Hormone levels in 6- to 8-month-old female and male Wt and ΔGLY-Adiponectin (Tg) mice where n = 5–10 per group in a controlled environment

	6- to 8-month-old females		6- to 8-month-old males	
	Wt	Tg	Wt	Tg
Fed glucose (mEq/liter)	162 ± 7	159 ± 6	175 ± 8	180 ± 7
Fasted glucose (mEq/liter)	118 ± 3	125 ± 4	135 ± 4	130 ± 3
Fed fatty acids (mEq/liter)	110 ± 10	105 ± 14	85 ± 13	109 ± 14
Fasted fatty acids (mEQ/liter)	210 ± 23	195 ± 24	220 ± 19	230 ± 16
Fed cholesterol (mg/dl)	152 ± 17	140 ± 10	147 ± 12	135 ± 11
Fasted cholesterol (mg/dl)	120 ± 9	111 ± 12	115 ± 8	110 ± 7
Fed lactate (mg/dl)	45 ± 8	40 ± 3	39 ± 5	42 ± 7

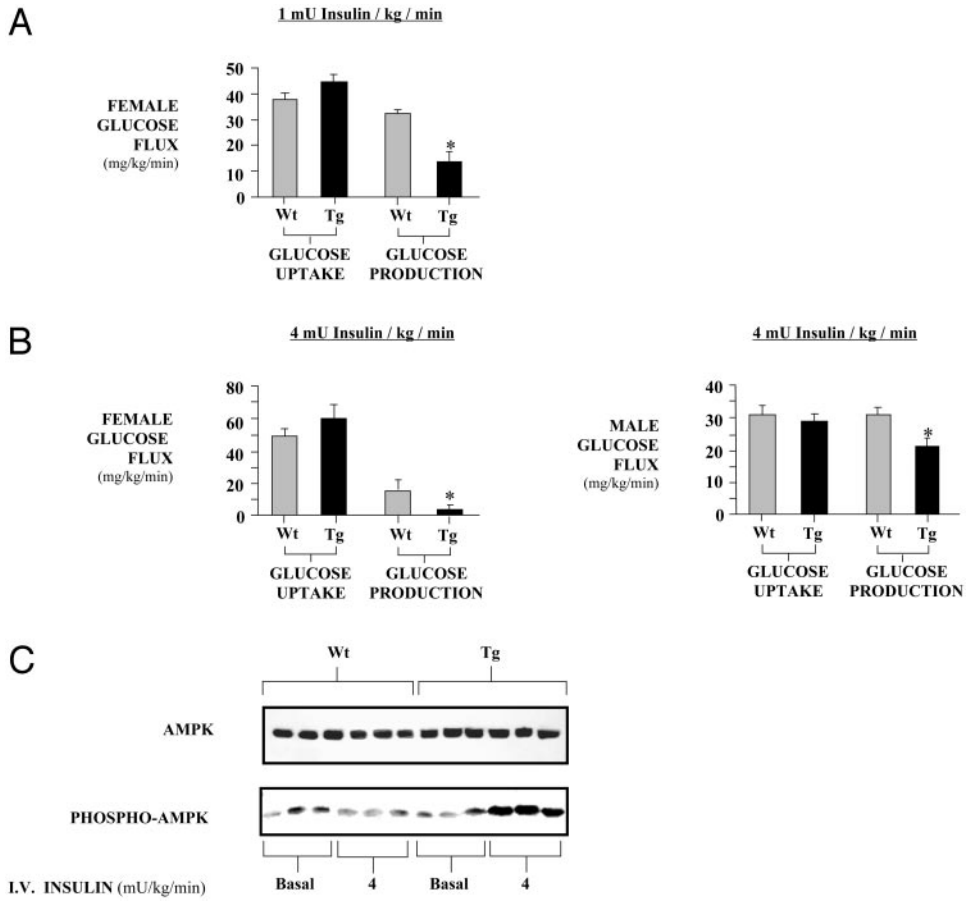

FIG. 10. Rate of glucose uptake and glucose production in 6- to 8-month-old female (A and B) and male (B) ΔGly-adiponectin mice (■) and their Wt littermates (▨) during clamps at low (A) and high (B) insulin levels. C, Phospho-AMPK and AMPK levels in liver extracts isolated from Wt and Tg female mice killed either under basal conditions (basal) or at the end of a hyperinsulinemic clamp study (4 mU/kg/min). In all cases, 50 μg liver protein were used for analysis. *, $P < 0.05$, Wt *vs.* Tg mice.

TABLE 4. Insulin clamp parameters in 6–8 month old female and male Wt and ΔGLY-Adiponectin (Tg) mice.

Insulin (mg/kg·h)	Sex	N		Body weight (g)		Basal insulin (ng/ml)		Liver lipid (% weight)	
		Wt	Tg	Wt	Tg	Wt	Tg	Wt	Tg
1.0	F	6	6	28.2 ± 1.5	32.7 ± 2.0	1.26 ± 0.31	*0.45 ± 0.14	N/A	N/A
4.0	F	3	3	32.1 ± 3.4	34.8 ± 1.6	1.43 ± 0.28	*0.67 ± 0.21	1.2 ± 0.2	1.6 ± 0.4
4.0	M	5	5	38.7 ± 3.6	37.8 ± 0.8	1.64 ± 0.31	*0.89 ± 0.35	1.4 ± 0.5	1.5 ± 0.1

F, Female; M, Male.

of cloned stromal preadipocytes. We have no evidence for an inhibitory activity on differentiation based on the expression of other differentiation-related marker proteins, such as resistin (3, 16), whose expression is, in fact, slightly elevated in fad pads from Tg animals. On the contrary, increased levels of adiponectin cause expansion of interscapular and orbital pads. The hyperproliferative response of the interscapular adipose tissue is not unique and has been reported previously. Tg overexpression of serum response element-binding protein-1c (SREBP-1c) in adipose tissue leads to development of a large fat mass in the interscapular region consisting of an enlarged, pale, bilobed fat pad highly similar in our mice (25, 26). These mice, in contrast to ours, are severely insulin resistant due to a generalized lipodystrophy, lack of leptin, and the presence of fatty livers.

Acute treatment of mice with thiazolidinediones has selective proliferative effects on interscapular brown adipocytes as well and increases UCP1 expression (27), eventually resulting in a very significant increase in adipose tissue in the interscapular region. These observations were recently also reported in both rats and monkeys treated with the potent PPARγ agonist darglitazone that resulted in hyperproliferation of a number of fat pads, in particular the dorsal thoracic and the interscapular brown adipose pads (28). It is noteworthy that thiazolidinediones also trigger a significant and sustained increase in circulating adiponectin levels, similar in magnitude to the increases achieved in our Tg model (12). Additional similarities to chronic PPARγ activation are found at the level of adipose tissue LPL induction that can be observed upon PPARγ agonist treatment (18) as well as in mice chronically overexpressing adiponectin, as demonstrated here. Interestingly, Wilson-Fritch and colleagues (29) recently reported that treatment of 3T3-L1 adipocytes with the PPARγ agonist rosiglitazone leads to a dramatic upregulation of a host of nuclear-encoded mitochondrial proteins, consistent with other observations made in WAT of rats and dogs that describe significant effects of rosiglitazone treatment on mitochondrial number and morphology (30).

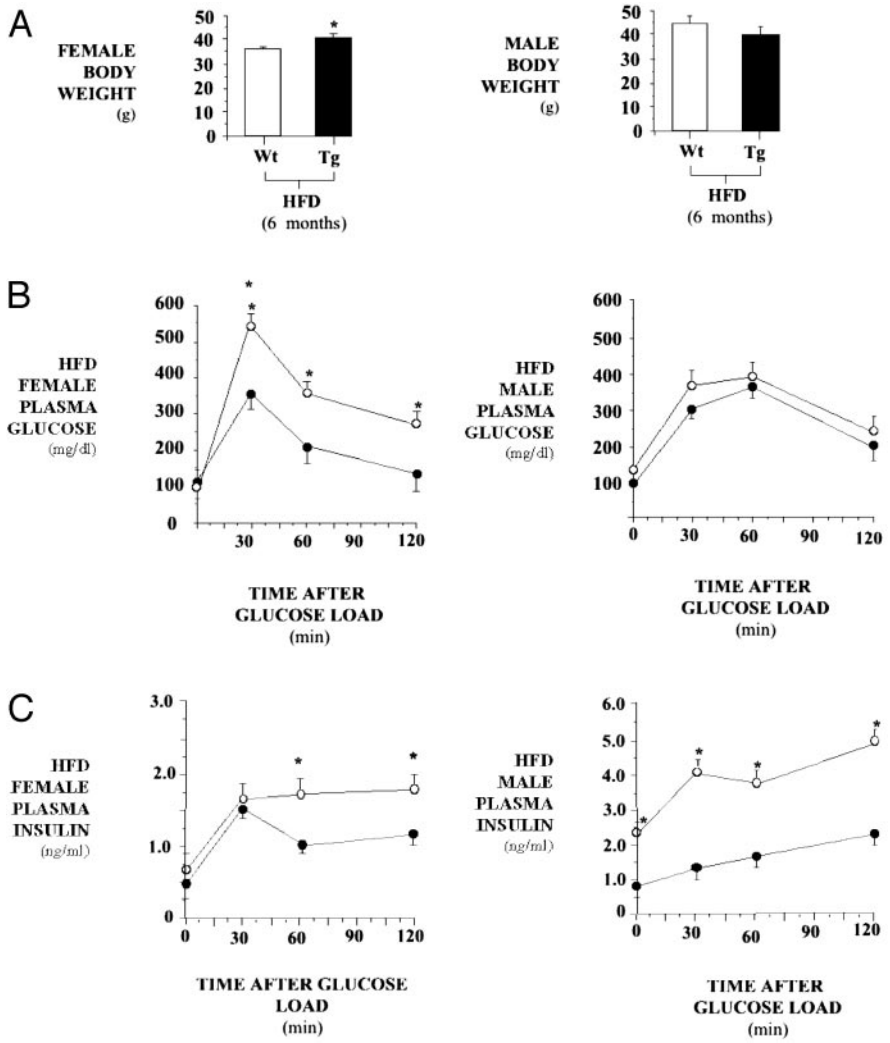

FIG. 11. A, Female and male body weights in Wt and ΔGly-adiponectin (Tg) mice after 6 months of a high fat diet initiated at weaning. B and C, Circulating glucose and insulin in 6-month-old high fat-fed female (*left*) and male (*right*) Tg mice (●) and their Wt littermates (○) after an oral glucose challenge. High fat feeding was initiated at weaning; mice were analyzed at 6 months of age. *, $P < 0.05$, Wt *vs.* Tg mice.

These increased levels of mitochondrial proteins may explain in part the ability of PPARγ agonists to increase β oxidation, which results in an increased clearance of free fatty acids that, in turn, can improve insulin sensitivity (31). Finally, even in humans there is an apparent propensity for hyperproliferation of a similar fat pad in the context of human immunodeficiency virus-mediated lipodystrophies, particularly in individuals undergoing highly aggressive antiretroviral therapy (HAART) (32, 33). There is, therefore, an increased propensity for the adipose tissue located in the interscapular region to undergo proliferation under a number of different conditions. Mechanistically, however, we do not know the link between serum response element-binding protein-1c overexpression in adipose tissue, thiazolidinedione-increased serum adiponectin levels, and human immunodeficiency virus protease inhibitors.

Orbital fat proliferation is a unique phenomenon among animal models. Only one other mouse model, the TSH receptor-induced model of Graves' ophthalmopathy, has displayed a similar phenotype, albeit on a much less dramatic scale (34). In this respect, our Tg mice recapitulate some phenotypic changes associated with Graves' exophthalmia. However, the Tg mice do not show evidence of hyperthyroidism or TSH receptor autoantibodies. It is therefore unlikely that the underlying causes of Graves' disease are directly linked to adiponectin overexpression. It is noteworthy that in a small cohort of Graves' patients displaying exophthalmos, we found serum adiponectin levels elevated by a factor of 2–3 above average levels and are currently testing whether the increased serum adiponectin is due to the hyperthyroidism *per se* (Combs, T. P., G. Baker, E. Ludgate, and P. E. Scherer, unpublished observations). Nevertheless, this suggests that the hypertrophy of the orbital fat pad observed in a subset of Graves' patients may be directly linked to the elevation of serum adiponectin, which, in turn, is secondary to a hormonal change induced by the autoimmune reaction. Consistent with that, a recent case has been reported in which a type 2 diabetic patient, upon initiation of treatment with the PPARγ agonist pioglitazone, experienced exacerbation of his thyroid eye disease, which had been stable and inactive for more then 2 yr. This patient displayed a massive expansion of the orbital fat pad (35).

This is the first time that orbital proliferation has been observed in mice to such a significant extent. Therefore, this mouse model offers a tool to study noninflammatory fat proliferation as often seen in Graves' ophthalmopathy.

It is surprising that the female Tg mice display such dramatic improvements in insulin sensitivity despite their increased adipose mass. Again, this phenomenon resembles the effects of thiazolidinedione treatment, which is known to lead to increases in serum adiponectin levels, insulin sensitivity, fat cell differentiation, and fat mass. Importantly, though, we ruled out the possibility that the improvement in insulin sensitivity is a secondary effect of the interscapular hyperproliferative fat pad, because we observed similarly striking improvements in insulin sensitivity in young male mice that showed no evidence of adipose depot redistribution.

In a very recent paper, Yamauchi and colleagues (36) reported the cloning of two receptors for adiponectin. Interestingly, one of these receptors shows preferential binding to the full-length native version of adiponectin and is predominantly expressed in the liver. The other receptor displays preferential binding to the globular trimeric version of adiponectin and shows a more ubiquitous tissue distribution, with strong expression in muscle. This is fully consistent with previous reports that show a differential effect of the two ligands on liver and muscle, respectively. It will be interesting to determine whether these receptors play any role in the differential adipose tissue distribution observed in the Tg mouse model presented here.

In summary, this is the first mouse model in which adiponectin levels are chronically elevated. This elevation is within physiological levels and accurately recapitulates the changes in endogenous adiponectin levels during maturation of the animal. These elevated serum adiponectin levels dramatically improve insulin sensitivity and at a later age lead to the hypertrophy of select fat pads. It is not clear whether this hypertrophy is the consequence of an autocrine effect of adiponectin or an indirect effect of improved systemic insulin sensitivity or is due to a hormonal change secondary to adiponectin overexpression. Consistent with our acute pharmacological studies, chronic elevation of full-length adiponectin in serum had a positive effect on insulin sensitivity, primarily in the liver. As several groups have implicated adiponectin as a possible mediator of thiazolidinedione action (12, 37–39), it is striking that chronic elevation of adiponectin by means of Tg overexpression causes effects that are vastly overlapping with those of chronic treatment with thiazolidinediones. This further strengthens the relationship between the effects of thiazolidinedione treatment and the induction of adiponectin as a prerequisite step to achieve clinical improvement in insulin sensitivity.

Acknowledgments

We are thankful to Dr. Rebecca Bahn (Mayo Clinic, Rochester, MN) for expert advice on various aspect of Graves' ophthalmopathy, Dr. James F. Nelson (University of Texas Health Science Center, San Antonio, TX) for help with the measurement of corticosterone, and Carolyn Marks and Leslie Cummins (AECOM) for help with the EM imaging.

Received August 18, 2003. Accepted October 7, 2003.

Address all correspondence and requests for reprints to: Dr. Philipp E. Scherer, Department of Cell Biology, Albert Einstein College of Medicine, 1300 Morris Park Avenue, Bronx, New York 10461. E-mail: scherer@aecom.yu.edu.

This work was supported by NIH National Research Service Award DK-61228 (to T.P.C.), NIH Hormones/Membrane Interactions Training Grant T32-DK-07513-15 (to T.P.C.), an American Diabetes Medical Scientist Training Grant (to A.H.B.), NIH Medical Scientist Training Grant T32-GM-07288 (to U.B.P. and M.W.R.), a postdoctoral fellowship from the Swiss National Science Foundation (to A.R.N.), a grant from the Wales Office for Research and Development (to G.B. and M.L.), the Core Laboratories of the Albert Einstein Diabetes Research and Training Center, NIH Grants R01-DK-45024 and R01-DK-48321 (to L.R.), and NIH Grants R01-DK-55758 and R03-EY-014935 (to P.E.S.).

References

1. **Havel, PJ** 2002 Control of energy homeostasis and insulin action by adipocyte hormones: leptin, acylation stimulating protein, and adiponectin. Curr Opin Lipidol 13:51–59
2. **Rajala MW, Scherer PE** 2003 Minireview: the adipocyte: at the crossroads of energy homeostasis, inflammation, and atherosclerosis. Endocrinology 144: 3765–3773
3. **Steppan CM, Bailey ST, Bhat S, Brown EJ, Banerjee RR, Wright CM, Patel HR, Ahima RS, Lazar MA** 2001 The hormone resistin links obesity to diabetes. Nature 409:307–312
4. **Berg AH, Combs T, Du X, Brownlee M, Scherer PE** 2001 The adipocyte-secreted protein Acrp30 enhances hepatic insulin action. Nat Med 7:947–953
5. **Hotta K, Funahashi T, Arita Y, Takahashi M, Matsuda M, Okamoto Y, Iwahashi H, Kuriyama H, Ouchi N, Maeda K, Nishida M, Kihara S, Sakai N, Nakajima T, Hasegawa K, Muraguchi M, Ohmoto Y, Nakamura T, Yamashita S, Hanafusa T, Matsuzawa Y** 2000 Plasma concentrations of a novel, adipose-specific protein, adiponectin, in type 2 diabetic patients. Arterioscler Thromb Vasc Biol 20:1595–1599
6. **Hotta K, Funahashi T, Bodkin NL, Ortmeyer HK, Arita Y, Hansen BC, Matsuzawa Y** 2001 Circulating concentrations of the adipocyte protein adiponectin are decreased in parallel with reduced insulin sensitivity during the progression to type 2 diabetes in rhesus monkeys. Diabetes 50:1126–1133
7. **Combs TP, Berg AH, Obici S, Scherer PE, Rossetti L** 2001 Endogenous glucose production is inhibited by the adipose-derived protein Acrp30. J. Clin. Inv. 108:1875–1881
8. **Fruebis J, Tsao TS, Javorschi S, Ebbets-Reed D, Erickson MR, Yen FT, Bihain BE, Lodish HF** 2001 Proteolytic cleavage product of 30-kDa adipocyte complement-related protein increases fatty acid oxidation in muscle and causes weight loss in mice. Proc Natl Acad Sci USA 98:2005–2010
9. **Maeda N, Shimomura I, Kishida K, Nishizawa H, Matsuda M, Nagaretani H, Furuyama N, Kondo H, Takahashi M, Arita Y, Komuro R, Ouchi N, Kihara S, Tochino Y, Okutomi K, Horie M, Takeda S, Aoyama T, Funahashi T, Matsuzawa Y** 2002 Diet-induced insulin resistance in mice lacking adiponectin/ACRP30. Nat Med 8:731–737
10. **Kubota N, Terauchi Y, Yamauchi T, Kubota T, Moroi M, Matsui J, Eto K, Yamashita T, Kamon J, Satoh H, Yano W, Nagai R, Kimura S, Kadowaki T, Noda T** 2002 Disruption of adiponectin causes insulin resistance and neointimal formation. J Biol Chem 277:25863–25866
11. **Yamauchi T, Kamon J, Waki H, Imai Y, Shimozawa N, Hioki K, Uchida S, Ito Y, Matsui J, Eto K, Komeda K, Tsunoda M, Murakami K, Ohnishi Y, Yamamura K, Ueyama Y, Froguel P, Kimura S, Nagai R, Kadowaki T** 2002 Globular adiponectin protected *ob/ob* mice from diabetes and apoE deficient mice from atherosclerosis. J Biol Chem 12:12
12. **Combs TP, Wagner JA, Berger J, Doebber T, Wang W-J, Zhang BB, Tanen M, Berg AH, O'Rahilly S, Savage DS, Chatterjee K, Weiss S, Larson PJ, Gottesdiener KM, Gertz BG, Charron MJ, Scherer PE, Moller DE** 2002 Induction of adipocyte complement-related protein of 30 kilodaltons by PPARγ agonists: a potential mechanism of insulin sensitization. Endocrinology 143:998–1007
13. **Lindemann D, Patriquin E, Feng S, Mulligan RC** 1997 Versatile retrovirus vector systems for regulated gene expression in vitro and in vivo. Mol Med 3:466–476
14. **Gossen M, Freundlieb S, Bender G, Muller G, Hillen W, Bujard H** 1995 Transcriptional activation by tetracyclines in mammalian cells. Science 268: 1766–179
15. **Engelman JA, Lisanti MP, Scherer PE** 1998 Specific inhibitors of p38 mitogen-activated protein kinase block 3T3-L1 adipogenesis. J Biol Chem 273:32111–32120
16. **Rajala MW, Lin Y, Ranalletta M, Yang XM, Qian H, Gingerich R, Barzilai N, Scherer PE** 2002 Cell type-specific expression and coregulation of murine resistin and resistin-like molecule-α in adipose tissue. Mol Endocrinol 16: 1920–1930
17. **Pajvani UB, Du X, Combs TP, Berg AH, Rajala MW, Schulthess T, Engel J, Brownlee M, Scherer PE** 2003 Structure-function studies of the adipocyte-secreted hormone Acrp30/adiponectin: implications for metabolic regulation and bioactivity. J Biol Chem 278:9073–9085
18. **Laplante M, Sell H, MacNaul KL, Richard D, Berger JP, Deshaies Y** 2003 PPAR-γ activation mediates adipose depot-specific effects on gene expression and lipoprotein lipase activity: mechanisms for modulation of postprandial lipemia and differential adipose accretion. Diabetes 52:291–299
19. **Shapiro L, Scherer PE** 1998 The crystal structure of a complement-1q family

protein suggests an evolutionary link to tumor necrosis factor. Curr Biol 8:335–338
20. **Combs TP, Berg AH, Rajala MW, Klebanov S, Iyengar P, Jimenez-Chillaron JC, Patti ME, Klein SL, Weinstein RS, Scherer PE** 2003 Sexual differentiation, pregnancy, calorie restriction and aging affect the adipocyte-specific secretory protein Acrp30/adiponectin. Diabetes 52:268–276
21. **Ludgate M, Baker G** 2002 Unlocking the immunological mechanisms of orbital inflammation in thyroid eye disease. Clin Exp Immunol 127:193–198
22. **Razani B, Combs TP, Wang XB, Frank PG, Park DS, Russell RG, Li M, Tang B, Jelicks LA, Scherer PE, Lisanti MP** 2002 Caveolin-1-deficient mice are lean, resistant to diet-induced obesity, and show hypertriglyceridemia with adipocyte abnormalities. J Biol Chem 277:8635–8647
23. **Yamauchi T, Kamon J, Minokoshi Y, Ito Y, Waki H, Uchida S, Yamashita S, Noda M, Kita S, Ueki K, Eto K, Akanuma Y, Froguel P, Foufelle F, Ferre P, Carling D, Kimura S, Nagai R, Kahn BB, Kadowaki T** 2002 Adiponectin stimulates glucose utilization and fatty-acid oxidation by activating AMP-activated protein kinase. Nat Med 8:1288–1295
24. **Yokota T, Meka CS, Medina KL, Igarashi H, Comp PC, Takahashi M, Nishida M, Oritani K, Miyagawa J, Funahashi T, Tomiyama Y, Matsuzawa Y, Kincade PW** 2002 Paracrine regulation of fat cell formation in bone marrow cultures via adiponectin and prostaglandins. J Clin Invest 109:1303–1310
25. **Shimomura I, Hammer RE, Richardson JA, Ikemoto S, Bashmakov Y, Goldstein JL, Brown MS** 1998 Insulin resistance and diabetes mellitus in transgenic mice expressing nuclear SREBP-1c in adipose tissue: model for congenital generalized lipodystrophy. Genes Dev 12:3182–3194
26. **Shimomura I, Hammer RE, Ikemoto S, Brown MS, Goldstein JL** 1999 Leptin reverses insulin resistance and diabetes mellitus in mice with congenital lipodystrophy. Nature 401:73–76
27. **Burkey BF, Dong M, Gagen K, Eckhardt M, Dragonas N, Chen W, Grosenstein P, Argentieri G, de Souza CJ** 2000 Effects of pioglitazone on promoting energy storage, not expenditure, in brown adipose tissue of obese *fa/fa* Zucker rats: comparison to CL 316,243. Metabolism 49:1301–1308
28. **Aleo MD, Lundeen GR, Blackwell DK, Smith WM, Coleman GL, Stadnicki SW, Kluwe WM** 2003 Mechanism and implications of brown adipose tissue proliferation in rats and monkeys treated with the thiazolidinedione darglitazone, a potent peroxisome proliferator-activated receptor-γ agonist. J Pharmacol Exp Ther 305:1173–1182
29. **Wilson-Fritch L, Burkart A, Bell G, Mendelson K, Leszyk J, Nicoloro S, Czech M, Corvera S** 2003 Mitochondrial biogenesis and remodeling during adipogenesis and in response to the insulin sensitizer rosiglitazone. Mol Cell Biol 23:1085–1094
30. **Toseland CD, Campbell S, Francis I, Bugelski PJ, Mehdi N** 2001 Comparison of adipose tissue changes following administration of rosiglitazone in the dog and rat. Diabetes Obes Metab 3:163–170
31. **Yu C, Chen Y, Cline GW, Zhang D, Zong H, Wang Y, Bergeron R, Kim JK, Cushman SW, Cooney GJ, Atcheson B, White MF, Kraegen EW, Shulman GI** 2002 Mechanism by which fatty acids inhibit insulin activation of insulin receptor substrate-1 (IRS-1)-associated phosphatidylinositol 3-kinase activity in muscle. J Biol Chem 277:50230–50236
32. **Qaqish RB, Fisher E, Rublein J, Wohl DA** 2000 HIV-associated lipodystrophy syndrome. Pharmacotherapy 20:13–22
33. **Gelato MC, Mynarcik DC, Quick JL, Steigbigel RT, Fuhrer J, Brathwaite CE, Brebbia JS, Wax MR, McNurlan MA** 2002 Improved insulin sensitivity and body fat distribution in HIV-infected patients treated with rosiglitazone: a pilot study. J Acquired Immune Defic Syndr 31:163–170
34. **Many MC, Costagliola S, Detrait M, Denef F, Vassart G, Ludgate MC** 1999 Development of an animal model of autoimmune thyroid eye disease. J Immunol 162:4966–4974
35. **Starkey K, Heufelder A, Baker G, Joba W, Evans M, Davies S, Ludgate M** 2003 Peroxisome proliferator-activated receptor-γ in thyroid eye disease: contraindication for thiazolidinedione use? J Clin Endocrinol Metab 88:55–59
36. **Yamauchi T, Kamon J, Ito Y, Tsuchida A, Yokomizo T, Kita S, Sugiyama T, Miyagishi M, Hara K, Tsunoda M, Murakami K, Ohteki T, Uchida S, Takekawa S, Waki H, Tsuno NH, Shibata Y, Terauchi Y, Froguel P, Tobe K, Koyasu S, Taira K, Kitamura T, Shimizu T, Nagai R, Kadowaki T** 2003 Cloning of adiponectin receptors that mediate antidiabetic metabolic effects. Nature 423:762–769
37. **Maeda N, Takahashi M, Funahashi T, Kihara S, Nishizawa H, Kishida K, Nagaretani H, Matsuda M, Komuro R, Ouchi N, Kuriyama H, Hotta K, Nakamura T, Shimomura I, Matsuzawa Y** 2001 PPARγ ligands increase expression and plasma concentrations of adiponectin, an adipose-derived protein. Diabetes 50:2094–2099
38. **Moore GB, Chapman H, Holder JC, Lister CA, Piercy V, Smith SA, Clapham JC** 2001 Differential regulation of adipocytokine mRNAs by rosiglitazone in *db/db* mice. Biochem Biophys Res Commun 286:735–741
39. **Yu JG, Javorschi S, Hevener AL, Kruszynska YT, Norman RA, Sinha M, Olefsky JM** 2002 The effect of thiazolidinediones on plasma adiponectin levels in normal, obese, and type 2 diabetic subjects. Diabetes 51:2968–2974

***Endocrinology* is published monthly by The Endocrine Society (http://www.endo-society.org), the foremost professional society serving the endocrine community.**